

Dynamic capacity allocation of hybrid transportation units for cargo-hitching in urban public transportation systems

Paul Bischoff¹, Benedikt Lienkamp¹, Tarun Rambha², and Maximilian Schiffer^{1,3}

¹School of Management, Technical University of Munich, Germany
paul.bischoff@tum.de, benedikt.lienkamp@tum.de

²Department of Civil Engineering & Center for Infrastructure, Sustainable Transportation and Urban Planning, Indian Institute of Science, Bengaluru, India
tarunrambha@iisc.ac.in

³ Munich Data Science Institute, Technical University of Munich, Germany
schiffer@tum.de

Abstract

To improve the utilization of public transportation systems (PTSs) during off-peak hours, we present an algorithmic framework that designs PTSs with hybrid transportation units (HTUs), which can transport passengers or freight by leveraging a flexible interior. Against this background, we study a capacitated network design problem to enable cargo-hitching in existing PTSs. Specifically, we study a setting with fixed vehicle routes and timetables in which vehicles can be equipped with HTUs to enable cargo-hitching. We optimize the network design from a total cost perspective to account for normalized network design costs tied to the investment in HTUs and freight routing costs. We present an algorithmic framework that encodes some of the problem's constraints in a spatially and temporally expanded, layered graph, and solves the resulting network design problem with a price-and-branch algorithm. We apply this framework to a case study based on the subway network in the city of Munich. Our algorithm outscales commercial solvers by a factor of six and yields integer feasible solutions with a median integrality gap of less than 1.02% for all instances. We show that cargo-hitching with HTUs increases the utilization of PTSs, especially during off-peak hours, without cannibalizing passenger service level and quality. Moreover, we present a sensitivity analysis that indicates that cargo-hitching is worthwhile if truck-based transport occurs at an externality cost of more than 1.6 € per vehicle and kilometer and loading and unloading costs of less than 2 € per passenger equivalent.

Keywords: capacitated network design, multi-commodity network flow, intermodal freight transportation, cargo-hitching

1. Introduction

As urban populations grow and cities become more interconnected, the demand for efficient public transit rises (United Nations 2019). Moreover, this population increase leads to significant growth of e-commerce transactions whose transportation contributes up to 15% of urban road transport (Dablanc 2011). As a consequence, cities suffer from overloaded transportation systems, whose negative externalities cause environmental harm via CO₂ emissions, health dangers via particulate matters and NO_x, and economic harm through working hours lost in congestion (Levy et al. 2010, Fattah et al. 2022). Focusing on freight transportation, electric vehicles and city freighters allow to reduce emission-related externalities. Focusing on passenger transportation, public transportation (PT) yields low costs per trip. Additionally, PT systems (PTS) offer sustainable mobility solutions as the emissions per passenger in a highly utilized PTS are significantly lower compared to individual mobility solutions (Noussan et al. 2022). So far, concepts discussed to realize sustainable transportation often focus either exclusively on freight or passenger transportation but share a central characteristic: the sustainability of each concept increases with greater utilization of its transportation modes. Still, for both freight and passenger transportation, concepts that allow to permanently maintain a high utilization are missing. PTSs in European cities show off-peak utilizations below 40% between 10 a.m. and 4 p.m. (Cheng et al. 2018, Chinn et al. 2020) and freight transport by design contains dead-headed driving, particularly when trucks or city freighters return to a depot.

To mitigate low PTS utilization during off-peak hours and relief heavily congested road networks partially occupied by freight trucks, this paper studies the concept of *cargo-hitching*, where a municipality equips its PTS such that it accommodates intermodal freight transportation without cannibalizing its primary purpose of offering convenient passenger transportation services. The concept promises a utilization increase of the PTS at zero additional installed capacity by using spare capacity available predominantly during off-peak hours. Furthermore, the utilization increase comes hand-in-hand with relieving congestion on roads because conventional truck-based deliveries can be reduced, which underlines the concept’s win-win nature.

Cargo-hitching has attracted practitioners’ attention over the last two decades. Although the first notable implementation *City Cargo* in Amsterdam was stopped primarily due to financing issues during the 2008 economic crisis (Arvidsson & Browne 2013), large urban PTS operators believe in the potential of the concept and fund its development and implementation (VGF 2021). For example, Figure 1 shows a recent and ongoing project, the *Gütertram* in Frankfurt am Main, Germany.

Figure 2 schematically shows a system in which a PTS operator can equip selected PT vehicles to accommodate both passenger and freight transportation, and can select PT stops to be used to exchange freight between logistic service providers (LSPs)’ vehicles and the equipped PT vehicles. As a result, freight deliveries pass a three-echelon system consisting of truck delivery to PT stops performed by LSPs, transportation in the PT vehicles performed

by the transit system operator, and last-mile delivery via city freighters again performed by LSPs.

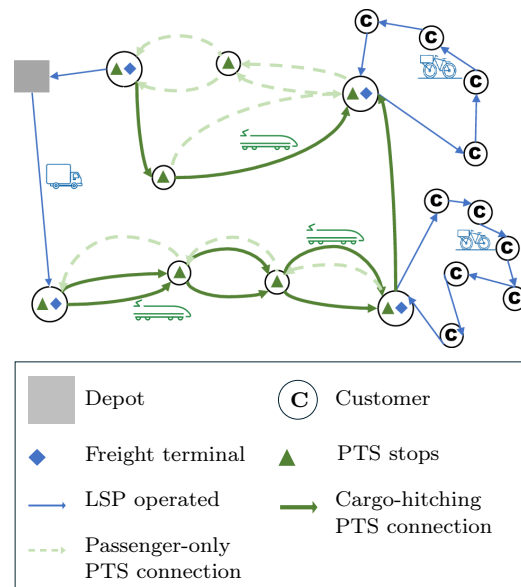
Contribution: We propose a novel urban cargo-hitching design problem that is, to the best of our knowledge, the first work to consider the dynamic allocation of PTS capacity in a multi-line PTSs. To solve real-world instances, we present a Price-and-branch (P&B) framework that relies on the following problem specific modifications to ensure scalability: first, it leverages a problem specific partially temporal and spatial graph expansion that allows to encode the complexity of some problem constraints in its graph structure. It further relies on an efficient pricing scheme that allows to decompose pricing problems by requests into shortest path problems (SPPs) that can be solved via the A^* algorithm. Moreover, we introduce multiple preprocessing techniques involving graph pruning and arc contraction that effectively decrease the cardinality of the arc set. To benchmark the performance of this algorithmic framework, we further provide a mixed integer program (MIP) formulation as well as a Branch-and-price (B&P) algorithm. Our framework utilizing the P&B approach solves instances with up to 3,000 requests on the subway network of Munich to a median integrality gap of 1.02% within computation times of 90 minutes. The proposed B&P algorithm improves the obtained median integrality gaps by additional 0.15 – 0.45 percentage points at the price of significantly increased computational cost. Both of our algorithmic solutions outscale a commercial solver by more than a factor of 6.

Beyond providing evidence on the computational efficiency of our framework, we derive several managerial insights based on our case study for the city of Munich. First, we show that cargo-hitching can offer a utilization increase at zero additional installed capacity. In this context, our algorithmic framework provides solutions that predominantly utilize the PTS’s off-peak hours to transport freight requests. Second, we show that the amount of freight

Figure 1: Practical implementation of cargo-hitching (Onomotion GmbH 2021)



Figure 2: Cargo-hitching system as three-echelon freight delivery via PTSs



transported via cargo-hitching is sensitive to the externality cost for truck-based delivery and the cost for (un-)loading freight into the PTS. In this context, our sensitivity analysis indicates that the full potential of cargo-hitching in the Munich subway network is realized if truck-based transport has externality costs of more than 1.6 € per vehicle and kilometer and loading and unloading costs are less than 2 € per passenger equivalent. Finally, we show that the savings realized by cargo-hitching depend on the spare capacity left within the PTS as well as the amount of freight requests that can be shipped through it. In this context, relying on hybrid transportation units (HTUs) to realize cargo-hitching is particularly beneficial if the amount of freight requests is high but the spare capacity left in the PTS fluctuates over the day due to passenger flow peaks.

Organization: The remainder of this paper is as follows. In Section 2, we summarize the state of the art. We then elaborate on our problem setting in Section 3 and develop our algorithmic framework in Section 4. Section 5 describes our case study based on the subway network in Munich, Germany. We present numerical results that show the efficiency of our algorithmic framework and derive managerial insights in Section 6. We conclude in Section 7 by summarizing our main findings.

2. State of the art

Exploring the potential of cargo-hitching relates back to the seminal work of Trentini & Malhene (2012). Early publications studied problem settings from an LSP perspective. Some works focussed on routing freight through a PTS without considering inter-dependencies to the preceding and succeeding vehicle routing tasks. In particular, Fatnassi et al. (2015), Behiri et al. (2018), and Ozturk & Patrick (2018) studied the scheduling of vehicles for freight transportation on a given network with fixed routes. Cheng et al. (2018) studied the matching of freight to services. Machado et al. (2023b) extended the assignment problem to a matching between requests on the one hand and stations and services on the other hand. Furthermore, Ma et al. (2023) considered a single-line co-modal urban PTS and provided operative time-invariant equilibrium conditions, such as fare prices and capacities. In contrast, Ghilas et al. (2016b) introduced the pickup and delivery problem with scheduled lines adapting the LSP perspective. They extended their work in further publications by providing an exact solution approach based on B&P (Ghilas et al. 2018) as well as a heuristic approach based on Adaptive Large Neighborhood Search (ALNS) (Ghilas et al. 2016a), and considered stochastic demands (Ghilas et al. 2016c). Other works studied related operational problem settings. Specifically, Masson et al. (2017) solved a two-tier vehicle routing problem (VRP) via ALNS in which they considered the PTS and subsequently the last-mile delivery via city freighters, Mandal & Archetti (2023) studied a three-tier VRP in which they additionally considered the transportation to the PTS and applied a decomposition method to solve it. We refer to Mourad et al. (2019) and Elbert & Rentschler (2022) for more details and recent advances on the operational aspects of cargo-hitching and related city logistic concepts. Instead, we

focus our discussion on the strategic aspects of node-based network design decisions, and the tactical and operational aspects of arc-based mode choices in the following.

Network design studies: Zhao et al. (2018) and Ji et al. (2020) formulated hub location problems (HLPs) in order to determine suitable PT stops to handle freight and demonstrated their approaches on the Shanghai network. However, both works neglected capacity restrictions at hubs. In contrast, El Ouadi et al. (2022) assign customers to suburban or urban bundling hubs with restricted hub capacities. However, the PT lines' capacities are unlimited, and flows are only considered at the hubs but not in the PTS. They applied machine learning to cluster zones and predict demands. Azcuy et al. (2021) studied a two-tier delivery system with a given PT capacity allocation, and minimized the expected travel distance performed by the last-mile vehicles. Thus, they derived strategic insights on PT stop locations from the solution of the operative VRP problem. Similarly, Delle Donne et al. (2023) determined suitable PT stops and PT lines, but still considered a simplified problem setting as the selected stops determine which PT lines can transport freight, i.e., no explicit capacity allocation decision happens at the vehicle level. Moreover, the problem setting remains time-invariant and ignores important transshipment and synchronization constraints. Nieto-Isaza et al. (2022) and Kızıl & Yıldız (2023) studied crowd-shipping delivery systems and strategically determined the locations of mini depots and satellites based on two-stage stochastic network design problems with stochastic demands. Although focusing on crowd-shipping, their problem setting shows parallels to our problem as they determine freight routes based on given network layouts and time-tables. However, they ignore the system operator's option to allocate capacities, and assume that PTS capacity is sufficient. Furthermore, Elbert et al. (2023) studied a combined hub location and service network design problem for long-haul rail transportation but discarded passenger flow-related constraints and assumed constant capacities.

Mode choice studies: Some works investigated the system operator's mode choices in co-modal PTSs but did not allow for the dynamic re-allocation of capacity. In this context, some works determined the sharing mode in cargo-hitching systems (Di et al. 2022), studied the scheduling of freight vehicles on fixed networks (Hörsting & Cleophas 2023), or assigned freight to fixed services (Machado et al. 2023a). Di et al. (2022) studied the joint optimization of train carriage arrangement and flow control. They determine the capacity allocation in terms of number of freight units to attach to every PT vehicle specifically during off-peak hours and, consequently, ignore the dynamic vehicle capacity re-allocation during operations. Moreover, Machado et al. (2023a) assumed that the demand for passenger transportation is known apriori and studied a stochastic problem in which uncertain freight demands are dropped into the left-over capacity of the PT bus system. Mostly, existing works consider two sharing modes: a *sharing-train mode* that allows passengers and freight to be transported in separate units of the same vehicle, and a *sharing-carriage mode* that allows passengers and shipments to share the same unit. Hörsting & Cleophas (2023) considered the sharing mode as an exogenous feature, and restricted the constant capacity accordingly. Li et al. (2023) determined the mode of each vehicle and the freight routes through the PTS. Al-

though similar to our problem setting with respect to the *sharing-train mode*, they allowed split freight routes which requires expensive unloading, sorting, and loading operations, and limits the works applicability in real-world settings. Moreover, their problem setting relies on a penalty to prevent the reduction of passenger level of service. Hence, they allow unlimited passenger service cannibalization if the benefits outweigh the penalties. Li et al. (2024) and Lin & Zhang (2024) neglect all strategic design aspects and investigate settings closest to our problem setting. Li et al. (2024) study the scheduling of passenger and freight underground units with semi-dynamic allocation of capacity. In their setting, a system operator can change the composition of underground trains in between trips at terminal stations. However, they do not enforce the prioritization of passengers over freight. Moreover, Lin & Zhang (2024) determine the number of transportation units in an underground system, their assignment to vehicles and the allocation of their capacity. Their work remains limited to a single line PT.

Conclusion: Table 1 shows the characteristics of the closest related works on network design and mode choices for cargo-hitching. As can be seen, no work exists that considers dynamic capacity allocation in a shared-vehicle setting when determining the network design of an urban cargo-hitching system. Notably, Di et al. (2022) and Li et al. (2023) considered a constant capacity allocation task by determining the sharing mode on the PT vehicle level but discarded other important characteristics. Li et al. (2024) and Lin & Zhang (2024) increased the flexibility of the capacity allocation task but discard all design aspects. Other works about cargo-hitching discarded the capacity allocation task even on a tactical level where capacity allocation is constant.

3. Problem setting

This work develops an algorithmic framework for the strategic planning tasks of a municipality to enable cargo-hitching in their PTS. To do so, the municipality needs to transform their PTS by adding two novel elements:

Table 1: Related works on quantitative strategic or tactical research on cargo-hitching.

	Behiri et al. (2018)	Ji et al. (2020)	Azcuy et al. (2021)	Di et al. (2022)	Delle Donne et al. (2023)	Nieto-Isaza et al. (2023)	Machado et al. (2022)	Ellbert et al. (2023a)	Li et al. (2023)	Hörsting & Cleophas (2023)	Lin & Zhang (2024)	Our work
Heterogeneous PT vehicles	✓	-	-	-	✓	-	✓	-	✓	-	-	✓
Freight transshipments	-	-	-	-	-	✓	-	-	✓	-	✓	✓
Time synchronization	✓	-	✓	✓	-	✓	✓	✓	✓	✓	✓	✓
Limited capacities	✓	-	✓	✓	✓	✓	✓	✓	✓	✓	✓	✓
Optional cargo-hitching	-	-	✓	✓	-	✓	-	✓	-	✓	-	✓
Passenger service level	✓	-	-	-	✓	✓	✓	-	✓	-	✓	✓
Capacity allocation	-	-	-	✓	-	-	-	-	✓	-	✓	✓

Freight terminals (FTs) are designated PT stops that allow the exchange of freight between a PTS and other means of transportation. At an FT, a truck can unload freight, which is then transported on a leg of the PTS, and unloaded at a different FT for last-mile delivery. Additionally, FTs allow storing and transshipping freight deliveries. The operations in FTs are automated with automated guided vehicles (AGVs) and are spatially separated from the passengers.

Hybrid transportation units (HTUs) allow transporting both freight and passengers. We focus on HTUs with a flexible interior that can be changed between trips to accommodate freight or passengers — but not both at the same time. For example, an HTU can be a specifically designed subway train wagon (cf. Kelly & Marinov 2017).

By replacing conventional wagons with HTUs, a municipality decides on the share of a PT vehicle that can be flexibly used for either freight or passenger transport. We note that this setting describes a special case of the *shared-vehicle* approach, which is particularly amenable for rail-based systems in which passengers and freight share the vehicle but not the wagon (Elbert & Rentschler 2022). Switching an HTU from passenger to freight transport or vice versa, e.g., by unfolding seats, requires little set-up time and can be automated. We restrict such mode changes to happen only at FTs due to practical constraints but allow for multiple functional switches of the HTUs during a day, such that the municipality can vary the share of freight capacities in the PTS between peak and off-peak hours to account for passenger demand.

We solve the municipalities’ strategic planning problem of deciding which PT lines and vehicles to equip with how many HTUs to minimize total freight transportation cost by allowing for cargo-hitching. We do not address the selection of suitable FTs but instead assume that the appropriate subset of PT stops has already been determined. The selected stops should offer sufficient space for freight operations and must be built at stops where PT schedules have a slightly longer stopover time. We explicitly consider passenger and freight transportation but prioritize passenger transportation to reflect concerns about limited acceptance of the concept that might arise if the current passenger service levels cannot be maintained. The resulting planning problem resembles a capacitated multi-commodity fixed-charge network design problem with an additional layer of complexity. The additional complexity arises from the capacity allocation decision between passengers and freight that leads to an additional integral dependency in which an HTU can accommodate freight or passengers but not both simultaneously. The operator determines the assignment of HTUs to PT vehicles and the dynamic allocation of flexible capacity from assigned HTUs to either passenger or freight. Additionally, the operator decides on the subset of freight requests that are accepted for transportation via the PTS, the subset of freight requests that are rejected, and the paths on which the passenger requests and the accepted freight requests are routed through the PTS.

We formally define the resulting planning problem in Section 3.1. Then, Section 3.2 formalizes the construction of our expanded graph representation that allows to encode certain

problem characteristics, and Section 3.3 provides a mixed integer program (MIP) formulation of our problem.

3.1. Problem definition

Formally, we consider a set of requests $\mathcal{R} = \mathcal{R}^P \cup \mathcal{R}^F$, which is the union of two distinct subsets: passenger requests \mathcal{R}^P and freight requests \mathcal{R}^F . Every request is defined as a quintuple $r = (o^r, d^r, q^r, e^r, l^r)$. Here, o^r denotes the request's origin, d^r its destination, q^r its demand, and e^r as well as l^r define the time interval $[e^r, l^r]$ in which the request must be processed, with e^r being the earliest start time and l^r marking the latest service completion time. The constraints on the service time apply to both passenger and freight requests. By adjusting a time window in one direction — specifically, by relaxing either e^r or l^r — we can adapt the less restrictive assumptions commonly used in works on flow assignment in public transit where either only a departure time or only an arrival time is given.

The PTS consists of a set of stops $s \in \mathcal{M}$. A subset of stops $\mathcal{Q} \subseteq \mathcal{M}$ serves as FTs. Moreover, a fleet of transit vehicles, denoted by \mathcal{H} , operates on this network with every transit vehicle $h \in \mathcal{H}$ following a specific sequence of stops. Each route corresponds to a PT vehicle's path through the PTS during the planning horizon and the times at which it services the constituent stops. We define a transit vehicles' route as a sequence of stops $\langle s_1, \dots, s_n \rangle$ with corresponding arrival times $\langle t_1, \dots, t_n \rangle$, where n represents the number of stops on that route. Accordingly, we define the route of a transit vehicle h as a sequence of tuples $L_h = \langle (s_1, t_1), \dots, (s_n, t_n) \rangle$ and the set of routes as $\mathcal{L} := \bigcup_{h \in \mathcal{H}} \{(s, t) : (s, t) \in L_h\}$. Every PT vehicle h consist of κ_h units with a unit capacity of λ_h . For the sake of subsequent discussions, we define $\mathcal{T}(s) := \langle t_1, t_2, \dots \rangle$ which contains all timesteps in which any vehicle arrives at a given stop $s \in \mathcal{M}$ as a sorted list of elements of $\{t : (s', t) \in \mathcal{L}, s' = s\}$ such that $t_u < t_{u'}, \forall u < u'$.

Decisions: The municipality services a given request $r \in \mathcal{R}$ by sending it from its origin o^r through the PTS to its destination d^r . Here, any possible connection from o^r to d^r is called a path $p \in \mathcal{P}(r)$ where $\mathcal{P}(r)$ denotes the set of all feasible paths servicing r . Every path can be represented as a sequence $p = \langle (o^r, e^r), (s_1, t_1), \dots, (s_q, t_q), (d^r, l^r) \rangle$ where q denotes the number of visited PT stops on path p . The municipality takes the following decisions:

- i) assigning an integer number $y_h \leq \kappa_h, y_h \in \mathbb{N}_0, h \in \mathcal{H}$ of HTUs to every PT vehicle. The remaining units can only transport passengers.
- ii) allocating an integer number $x_{(s_i, t_i), (s_j, t_j)} \leq y_h, x_{(s_i, t_i), (s_j, t_j)} \in \mathbb{N} \cup \{0\}$ of HTUs to transporting freight between two consecutive freight terminals $(s_i, t_i), (s_j, t_j) \in L_h, s_i, s_j \in \mathcal{Q}$ on every vehicles' route L_h . We implicitly assume either zero or a minimum of 2 FTs on every vehicle's route.
- iii) selecting a subset of freight requests accepted for transportation via the PTS.
- iv) assigning flows $0 \leq g_p^r \leq q^r, r \in \mathcal{R}^P, p \in \mathcal{P}(r)$ that determine one or multiple paths to partially service the respective passenger request. Note that we allow the split of flows to reflect the various journey patterns of individual passengers.

- v) assigning flows $f_p^r \in \{0, q^r\}$, $r \in \mathcal{R}^F$, $p \in \mathcal{P}(r)$ that determine a singular feasible path for every accepted freight request.

Solution: A feasible, well-defined solution adheres to the following constraints:

- i) it preserves a passenger service level $\chi \in [0, 1]$ ensuring that an exogenously given share of passenger demand is serviced, i.e., $\sum_{r \in \mathcal{R}^P} \sum_{p \in \mathcal{P}(r)} g_p^r \geq \chi \sum_{r \in \mathcal{R}^P} q^r$ holds.
- ii) it respects the passenger capacity of every PT vehicle at all times. The passenger capacity is determined by the status quo adjusted by the capacity allocated to freight transportation, i.e., $\lambda_h(\kappa_h - x_{(s_i, t_i), (s_j, t_j)})$, $h \in \mathcal{H}$. Here, s_i, s_j denote any pair of consecutive FTs on the respective vehicle's route L_h .
- iii) it respects the freight capacity of every PT vehicle at all times. The freight capacity is determined by the allocated HTU decision, i.e., the capacity between any pair of consecutive FTs s_i, s_j on a vehicle's route L_h is $\lambda_h x_{(s_i, t_i), (s_j, t_j)}$, $h \in \mathcal{H}$.

Objective: The municipality aims to minimize the total system cost with respect to cargo-hitching adoption. This cost entails multiple components:

- i) a design cost $c_h > 0$ per HTU that is assigned to vehicle $h \in \mathcal{H}$ representing the normalized investment cost that is scaled to the investigated time period.
- ii) a penalty cost $c_{\text{PEN}}^r > 0$ for every freight request $r \in \mathcal{R}^F$ rejected by the municipality and representing the cost of negative externalities due to conventional truck delivery.
- iii) a routing cost $c_{s_i, s_{i+1}} > 0$ per unit freight or passenger that the PTS transports between consecutive stops $s_i, s_{i+1} \in \mathcal{M}$ on any vehicle h 's route L_h .

Note that we do not account for passenger transportation costs in the objective because cost differences between passenger paths of acceptable quality are marginal.

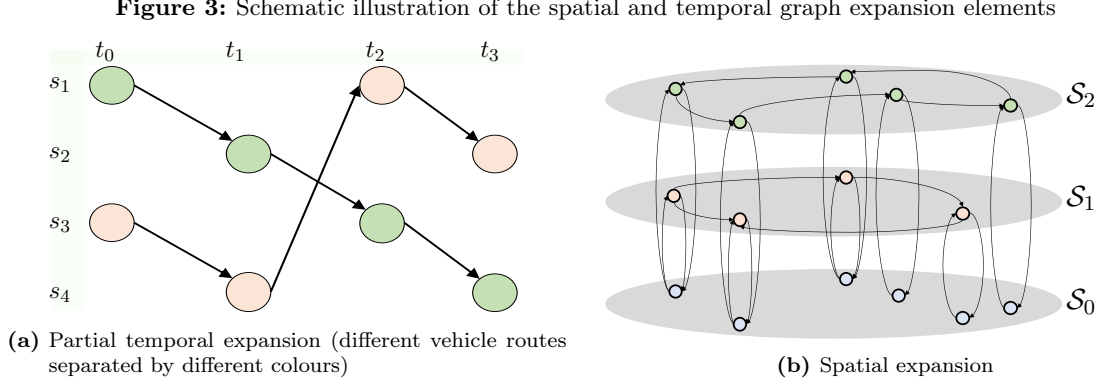
3.2. Expanded graph construction

To devise an effective algorithm, we encode some of the problem's temporal and spatial complexity by using a problem-specific graph representation. Specifically, we use a temporal graph expansion in which vertices represent a combination of location and time (cf. Figure 3a) and combine it with a spatial expansion in which we separate different vehicles' routes through the PTS into $|\mathcal{H}| + 1$ different graph layers (cf. Figure 3b). The expanded graph contains one separate layer of temporally expanded vertices for every vehicle $h \in \mathcal{H}$, and one additional layer that we refer to as holding layer. We denote the resulting multi-layered graph with its vertex and arc sets as $G = (\mathcal{V}, \mathcal{A})$. We finish the formal construction of G by providing an example at the end of this section.

Vertex set construction: Let $\mathcal{T} := \bigcup_{r \in \mathcal{R}} (e^r \cup l^r) \cup \bigcup_{s \in \mathcal{M}} \mathcal{T}(s)$ be the set of all relevant timesteps in a given problem instance. Furthermore, let the vertex set $\mathcal{V} := \mathcal{S} \cup \mathcal{O} \cup \mathcal{D}$ be the union of the subsets \mathcal{S} , \mathcal{O} , and \mathcal{D} , which we define one-by-one in the remainder of this section.

First, we obtain \mathcal{O} and \mathcal{D} by expanding each request's origin and destination into the time dimension. Thus, $\mathcal{O} := \bigcup_{r \in \mathcal{R}} (o^r, e^r)$ and $\mathcal{D} := \bigcup_{r \in \mathcal{R}} (d^r, l^r)$.

Second, we describe a vertex $v \in \mathcal{S}$ as a temporal node represented by a triplet that links a physical location $s \in \mathcal{M}$ to a specific timestep $t \in \mathcal{T}$ and a specific graph layer $\{0\} \cup \mathcal{H}$.



Accordingly, we define sets $\mathcal{S}_h := \{(s, t, h) : (s, t) \in L_h\}$, $h \in \mathcal{H}$ as the vertices at which vehicle h arrives at stop s at timestep t . This is a partial time expansion in which only the relevant points in time are expanded (cf. Boland et al. 2017). Here, every set \mathcal{S}_h denotes the vertices of a different vehicle layer. Additionally, we introduce a specific holding layer vertex set $\mathcal{S}_0 := \{(s, t, 0) : (s, t) \in \mathcal{L}\}$ that contains one additional copy per stop s and timestep t in which a vehicle arrives at s . The holding layer connects the vehicle layers and orchestrates the time synchronization of transfers and transshipments. Finally, we define $\mathcal{S} := \mathcal{S}_0 \cup \bigcup_{h \in \mathcal{H}} \mathcal{S}_h$ as the set of all temporally expanded vertices that represent stops across all graph layers. In the expanded graph, we refer to the set of FT representations as $\mathcal{B} := \{(s, \cdot, \cdot) \in \mathcal{S} : s \in \mathcal{Q}\}$.

Arc set construction: We create the resulting graph's arc set \mathcal{A} in a top-down manner. More specifically, we derive the set of arcs \mathcal{A} in the expanded graph G as the union of multiple disjoint arc subsets, i.e., $\mathcal{A} := \mathcal{A}^V \cup \mathcal{A}^0 \cup \mathcal{A}^T \cup \mathcal{A}^A \cup \mathcal{A}^E$.

Vehicle arcs $(i, j) \in \mathcal{A}^V$ complete the vehicle layer vertex sets in the multi-layered graph G and represent the PT vehicles' routes. We define the set $\mathcal{A}^V := \bigcup_{h \in \mathcal{H}} \mathcal{A}_h$ as the union of temporal arc sets \mathcal{A}_h that contain the arcs representing the route of vehicle $h \in \mathcal{H}$ in its corresponding graph layer. Here, we construct the arcs $(i, j) \in \mathcal{A}_h$ such that they connect consecutive stops $(s_l, t_l), (s_{l+1}, t_{l+1})$ on a vehicle's route L_h . More formally, we construct arcs $(i, j) \in \mathcal{A}_h$ such that $i = (s_l, t_l, h) \in \mathcal{S}_h$, $j = (s_{l+1}, t_{l+1}, h) \in \mathcal{S}_h$, $l \in \{1, \dots, n-1\}$.

The arc set \mathcal{A}^0 is the set of holding arcs that enable holding requests at stops of the PTS, i.e., passengers or freight waiting at a stop. Let u be the index of the ordered set of times $\mathcal{T}(s)$ in which any vehicle arrives at stop s . Then, we create holding arcs $(i, j) \in \mathcal{A}^0$ where $i = (s, t_u, 0) \in \mathcal{S}_0$ and $j = (s, t_{u+1}, 0) \in \mathcal{S}_0$, for all $s \in \mathcal{M}$, $t_u, t_{u+1} \in \mathcal{T}(s)$, and $u = 1, \dots, |\mathcal{T}(s)| - 1$. Thus, we connect vertices in the holding layer vertex set that are copies of the same physical stop location $s \in \mathcal{M}$ such that two connected vertices represent two consecutive timesteps $t_u, t_{u+1} \in \mathcal{T}(s)$ in which a PT vehicle arrives at the respective stop.

To connect the disjunct vertex sets of the different layers, we add transit arcs $(i, j) \in \mathcal{A}^T$. Here, we connect temporal vertices $i = (s, t, h) \in \mathcal{S}_h$, $h \in \mathcal{H}$ with their corresponding representation in the holding layer $j = (s, t, 0) \in \mathcal{S}_0$. This is a many-to-one mapping as multiple vertices in the vehicle layer vertex set may share the same representation in the holding layer, e.g., if they represent the same physical stop at the same timestep. To establish this mapping in a bidirectional fashion, we further add the inverse arc (j, i) .

Moreover, we connect the temporal vertices $i = (o^r, e^r) \in \mathcal{O}, r \in \mathcal{R}^P$ with the PTS at vertices $j = (s, t, 0) \in \mathcal{S}_0$ by arcs $(i, j) \in \mathcal{A}^A$. Accordingly, we connect the temporal vertices $i = (o^r, e^r) \in \mathcal{O}, r \in \mathcal{R}^F$ with the PTS at vertices $j = (s, t, 0) \in \mathcal{S}_0 \cap \mathcal{B}$ by additional arcs $(i, j) \in \mathcal{A}^A$. Finally, we construct arcs $(i, j) \in \mathcal{A}^E$ that connect the PTS vertices $i = (s, t, 0) \in \mathcal{S}_0$ with the temporal destinations $j = (d^r, l^r) \in \mathcal{D}, r \in \mathcal{R}^P$ and additional arcs $(i, j) \in \mathcal{A}^E$ that connect the PTS vertices $i = (s, t, 0) \in \mathcal{S}_0 \cap \mathcal{B}$ with the temporal destinations $j = (d^r, l^r) \in \mathcal{D}, r \in \mathcal{R}^F$. Here, we prune the graph based on distance and time thresholds as outlined in Appendix D.

Preprocessing: We apply multiple preprocessing steps to encode problem characteristics in G , which reduces the size and the computational complexity of the MIP formulation in Section 3.3.

First, we encode the system operator's acceptance decisions on transporting freight requests $r \in \mathcal{R}^F$ into the expanded and multi-layered graph by constructing dummy arcs $(i, j) \in \mathcal{A}^D \subset \mathcal{A}$ such that the decision to reject a freight request r corresponds to routing it through the network on a dummy arc. Formally, we add dummy arcs $(i, j) \in \mathcal{A}^D$, with $i = (o^r, e^r)$ and $j = (d^r, l^r)$ for all $r \in \mathcal{R}^F$ and assign the arc cost $c_{i,j} = \frac{1}{q^r} c_{\text{PEN}}^r$ such that the encoded routing cost equals the penalty cost from rejecting a request. Because we enforce binary freight flows, we can decode the decision to accept or reject a request from the network flow without further intricacies.

Second, to reduce the problem's complexity, we aim at decreasing the cardinality of the arc set. Furthermore, the required capacity for freight transportation remains stable at PT stops that are not FTs, i.e., $\forall s \in \mathcal{M} \setminus \mathcal{Q}$ as no freight can enter or leave the PTS at such stops. We leverage this observation and further abstract the PTS by constructing freight path segment arcs that connect consecutive FTs on every vehicle's route — thereby contracting multiple arcs into a single arc. Let $m \geq 1$, where $m - 1$ is the number of PT stops between the two consecutive freight terminals. Furthermore, let $i = (s_l, t_l, h) \in \mathcal{S}_h \cap \mathcal{B}$ and $j = (s_{l+m}, t_{l+m}, h) \in \mathcal{S}_h \cap \mathcal{B}$ be the two vertices in the vehicle layer of a vehicle h representing the two consecutive FTs on the vehicle's route. Formally, $(s_l, t_l), (s_{l+m}, t_{l+m}) \in L_h$ such that $\nexists (s_{l+p}, t_{l+p}) \in L_h : 0 < p < m, s_{l+p} \in \mathcal{Q}$. For all such i, j , we add the freight path segment arcs $(i, j) \in \mathcal{A}^F \subset \mathcal{A}$. Here, we make sure that costs are consistent by setting $c_{i,j} = \sum_{p=1}^m c_{s_{l+p-1}, s_{l+p}}$.

Third, we pre-compute sets of passenger paths $\mathcal{P}(r), r \in \mathcal{R}^P$ (cf. Li et al. 2024). Thus, we can ensure suitable passenger service criteria based on the pre-computed sets by filtering for the chosen criteria, e.g., filtering for paths that induce a maximum number of transfers or using specific modes in a multi-modal setting. Hence, we reduce the problem's computational complexity by converting the minimum cost network flow problem for passengers into a relaxed fractional set covering problem.

Graph expansion example: The following provides an illustrative example of a PTS and its graph representation. In this example, the PTS consists of two vehicles $\mathcal{H} = \{1, 2\}$ operating the following routes: $\mathcal{L}_1 = \langle (s_1, 2), (s_2, 3), (s_3, 4), (s_4, 6) \rangle$ and $\mathcal{L}_2 = \langle (s_5, 1), (s_2, 2), (s_3, 3), (s_6, 4) \rangle$. We assume the set of FTs to be $\mathcal{Q} = \{s_1, s_2, s_4, s_5, s_6\}$,

and consider two requests $\mathcal{R} = \{1, 2\}$, both of which come with a demand of $q^1 = q^2 = 1$. Request $1 \in \mathcal{R}^P$ is a passenger request, and the corresponding group of passengers wants to start their itinerary no earlier than time $t = 0$ and finish it before or at $t = 5$. Freight request $2 \in \mathcal{R}^F$ can leave its origin no earlier than time 0 and must be fulfilled with $t = 6$. Figure 4 shows the corresponding expanded graph. In the preprocessing, we have added dummy arc $((o^1, 0), (d^1, 5)) \in \mathcal{A}^D$ as well the freight path segments $((s_1, 2, 1), (s_2, 3, 1)), ((s_2, 3, 1), (s_4, 6, 1)), ((s_5, 1, 2), (s_2, 2, 2)), ((s_2, 2, 2), (s_6, 4, 2)) \in \mathcal{A}^F$.

3.3. MIP formulation

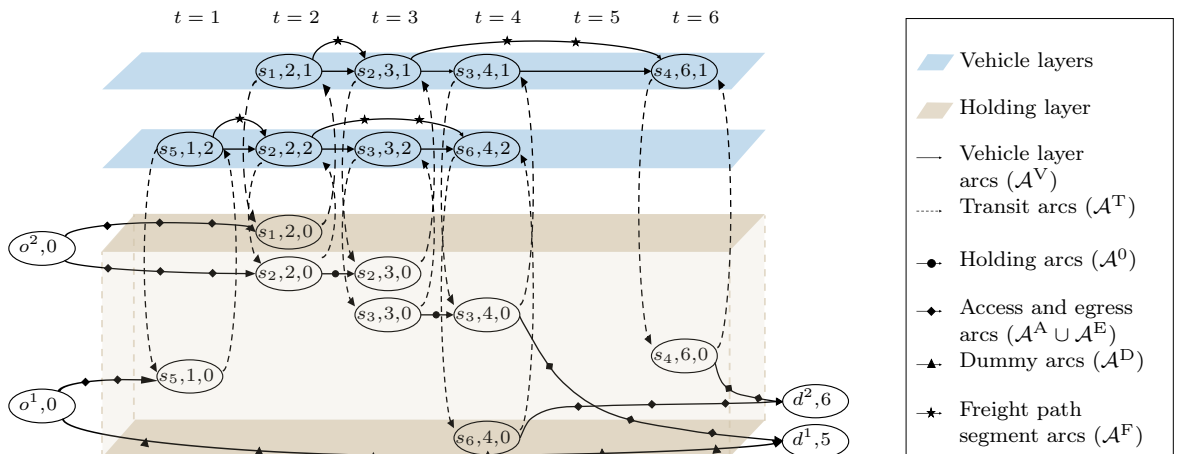
Based on the expanded, multi-layered, and pre-processed graph $G = (\mathcal{V}, \mathcal{A})$ introduced in Section 3.2, we formulate the problem as a MIP in this section. In Appendix A, we provide a tabular summary of notation. For the ease of notation, we first explicitly define the arc set $\mathcal{A}^C \subseteq \mathcal{A}$ that we consider when determining freight flows. This arc set contains the freight path segments \mathcal{A}^F , the dummy arcs \mathcal{A}^D , the connections between FT representations from \mathcal{A}^T and \mathcal{A}^0 , and the relevant connections of origins and destinations with the PTS. More formally,

$$\begin{aligned} \mathcal{A}^C := & \mathcal{A}^F \cup \mathcal{A}^D \cup \{((o^r, e^r), (s, t, 0)) \in \mathcal{A}^A : r \in \mathcal{R}^F\} \cup \\ & \{((s, t, 0), (d^r, l^r)) \in \mathcal{A}^E : r \in \mathcal{R}^F\} \cup \\ & \{(i, j) \in \mathcal{A}^0 \cup \mathcal{A}^T : i, j \in \mathcal{B}\} \end{aligned}$$

Note that a graph decomposition by commodity type, i.e., passenger and freight, is not straightforward because both commodities share a total capacity that needs explicit allocation. We define the vertex demand ξ_i^r , $i \in \mathcal{V}, r \in \mathcal{R}^F$ describing the difference between total inflow and total outflow of a specific request in a vertex as

$$\xi_i^r = \begin{cases} 1, & \text{if } i = (o^r, e^r), \\ -1, & \text{if } i = (d^r, l^r), \\ 0 & \text{otherwise.} \end{cases}$$

Figure 4: Illustrative example of a partial temporal expanded, multi-layered, and preprocessed graph



In this context, we restrict the vertex sets $\mathcal{N}(i)$ to neighboring vertices of vertex i that are directly connected via arcs from \mathcal{A}^C , i.e., arcs that allow for freight transportation. Formally, $\mathcal{N}^+(i) := \{j \in \mathcal{V} : (i, j) \in \mathcal{A}^C\}$ and $\mathcal{N}^-(i) := \{j \in \mathcal{V} : (j, i) \in \mathcal{A}^C\}$, respectively. We refer by $\mu : \mathcal{A}^V \rightarrow \mathcal{A}^F \cup \emptyset$ to the many-to-one mapping function that assigns a contracted arc to its corresponding freight path segment. Some arcs in the vehicle layers might not be contracted. Therefore, we differentiate between arcs from the vehicle layer arc set that are contracted and arcs that are not being contracted. Here, $\mathcal{I} := \{(i, j) \in \mathcal{A}^V : \mu(i, j) \neq \emptyset\}$ denotes the contracted arcs, and vice versa $\mathcal{J} = \{(i, j) \in \mathcal{A}^V : \mu(i, j) = \emptyset\}$ denotes the arcs that are not contracted. In Figure 5, we present a simplified illustration of this formalization with six temporal vertices, of which only three represent FTs. Table 2 demonstrates the resulting arc sets. Finally, using the introduced notation, we can formulate the problem as a MIP as follows

$$\min_{y, x, g, f} \sum_{h \in \mathcal{H}} c_h y_h + \sum_{r \in \mathcal{R}^F} q^r \sum_{(i, j) \in \mathcal{A}^C} c_{i, j} f_{i, j}^r \quad (1a)$$

s.t.

$$\sum_{r \in \mathcal{R}^P} \sum_{p \in \mathcal{P}(r)} q^r g_p^r \geq \chi \sum_{r \in \mathcal{R}^P} q^r, \quad (1b)$$

$$\sum_{j \in \mathcal{N}^+(i)} f_{i, j}^r - \sum_{j \in \mathcal{N}^-(i)} f_{j, i}^r = \xi_i^r, \quad \forall r \in \mathcal{R}^F, i \in \mathcal{O} \cup \mathcal{D} \cup \mathcal{B}, \quad (1c)$$

$$\sum_{r \in \mathcal{R}^P} \sum_{p \in \mathcal{P}(r)} q^r g_p^r \theta_{i, j}^p \leq \sum_{h \in \mathcal{H}} \omega_{i, j}^h \lambda_h (\kappa_h - x_{\mu(i, j)}), \quad \forall (i, j) \in \mathcal{I}, \quad (1d)$$

$$\sum_{r \in \mathcal{R}^P} \sum_{p \in \mathcal{P}(r)} q^r g_p^r \theta_{i, j}^p \leq \sum_{h \in \mathcal{H}} \omega_{i, j}^h \lambda_h \kappa_h, \quad \forall (i, j) \in \mathcal{J}, \quad (1e)$$

$$\sum_{r \in \mathcal{R}^F} q^r f_{i, j}^r \leq \sum_{h \in \mathcal{H}} \omega_{i, j}^h \lambda_h x_{i, j}, \quad \forall (i, j) \in \mathcal{A}^F, \quad (1f)$$

$$\sum_{p \in \mathcal{P}(r)} g_p^r \leq 1, \quad \forall r \in \mathcal{R}^P, \quad (1g)$$

$$x_{i, j} \leq \sum_{h \in \mathcal{H}} \omega_{i, j}^h y_h, \quad \forall (i, j) \in \mathcal{A}^F, \quad (1h)$$

$$y_h \leq \kappa_h, \quad \forall h \in \mathcal{H}, \quad (1i)$$

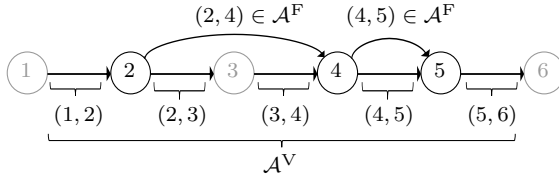
$$g_p^r \geq 0, \quad \forall r \in \mathcal{R}^P, p \in \mathcal{P}(r), \quad (1j)$$

$$f_{i, j}^r \in \{0, 1\}, \quad \forall r \in \mathcal{R}^F, (i, j) \in \mathcal{A}^C, \quad (1k)$$

$$y_h \in \mathbb{N}_0, \quad \forall h \in \mathcal{H}, \quad (1l)$$

$$x_{i, j} \in \mathbb{N}_0, \quad \forall (i, j) \in \mathcal{A}^F \quad (1m)$$

The Objective (1a) minimizes freight transportation costs, which entail investment cost for HTUs to design a network with flexible capacities, constant penalty terms for rejected freight requests, encoded as a routing cost on the arc subset $\mathcal{A}^D \subset \mathcal{A}^C$, and variable costs for every unit of freight flow transported via the PTS. Constraint (1b) ensures the demand-weighted passenger service level. Constraints (1c) impose classical flow conservation for every freight request $r \in \mathcal{R}^F$. Constraints (1d) and (1e) ensure that the system capacity in terms

Figure 5: Arc contraction illustration**Table 2:** Arc contraction sets

Set	Elements
\mathcal{I}	$(2, 3), (3, 4), (4, 5)$
\mathcal{J}	$(1, 2), (5, 6)$

of passengers is respected on the contracted arcs and the non-contracted arcs, respectively. Constraints (1f) restrict the freight flow per arc $(i, j) \in \mathcal{A}^F$ depending on the number of HTUs whose capacities are allocated to freight transportation on the respective freight path segment. Constraints (1g) restrict the passenger flow per request to one. Constraints (1h) and (1i) limit the number of HTUs allocated for freight transportation. Specifically, Constraints (1h) restrict this number to the HTUs assigned to vehicle $h \in \mathcal{H}$, while Constraints (1i) limit the number of HTUs to the maximum number of units κ_h available. Finally, Constraints (1j) - (1m) define the domains of the decision variables.

4. Algorithm

We propose a P&B solution method to find integer feasible solutions to Problem 1. First, we reformulate Problem 1 as a path-based formulation in Section 4.1. Second, we detail our P&B approach in Section 4.2. Finally, we provide a B&P method as an alternative to our P&B algorithm in Section 4.3.

4.1. Path-based reformulation

Let z_p^r denote the fraction of demand q^r , $r \in \mathcal{R}^F$ that is transported via path $p \in \mathcal{P}(r)$. The path-based formulation required to apply Column Generation (CG) reads

$$\min_{y, x, g, z} \sum_{h \in \mathcal{H}} c_h y_h + \sum_{r \in \mathcal{R}^F} \sum_{p \in \mathcal{P}(r)} \sum_{(i,j) \in \mathcal{A}^C} q^r c_{i,j} \theta_{i,j}^p z_p^r \quad (2a)$$

s.t.

$$(\alpha) \quad \sum_{r \in \mathcal{R}^F} \sum_{p \in \mathcal{P}(r)} q^r \theta_{i,j}^p z_p^r \leq \sum_{h \in \mathcal{H}} \omega_{i,j}^h \lambda_h x_{i,j}, \quad \forall (i,j) \in \mathcal{A}^F, \quad (2b)$$

$$(\eta) \quad \sum_{p \in \mathcal{P}(r)} z_p^r = 1, \quad \forall r \in \mathcal{R}^F, \quad (2c)$$

$$z_p^r \in \{0, 1\}, \quad \forall r \in \mathcal{R}^F, p \in \mathcal{P}(r) \quad (2d)$$

adhering further to Constraints 1b, 1d - 1e, 1g - 1j, and 1l-1m. In the continuous relaxation of Problem 2 each set of constraints is associated with a set of dual variables. Here, the dual variables $\alpha_{i,j} \in \mathbb{R}_0^-$, $(i, j) \in \mathcal{A}^F$ are associated with Constraints 2b limiting the freight flow on the respective arcs. Constraints 2c enforce the sum of all freight flows per request to be equal to one. Thus, the associated dual variables $\eta^r \in \mathbb{R}$, $r \in \mathcal{R}^F$ are free. Moreover, the dual variable $\gamma \in \mathbb{R}_0^+$ is associated with the service level Constraint 1b. The dual variables $\nu_{i,j} \in \mathbb{R}_0^-$, $(i, j) \in \mathcal{I}$ and $\nu_{i,j} \in \mathbb{R}_0^-$, $(i, j) \in \mathcal{J}$ are associated with the passenger capacity limiting

Constraints 1e, and Constraints 1d respectively. Additionally, dual variables $\delta^r \in \mathbb{R}_0^-$, $r \in \mathcal{R}^P$ are associated with Constraints 1g, dual variables $\pi_{i,j} \in \mathbb{R}_0^-$, $(i,j) \in \mathcal{A}^F$ are associated with Constraints 1h, and dual variables $\tau_h \in \mathbb{R}_0^-$, $h \in \mathcal{H}$ are linked to Constraints 1i. Based on the path-based Problem 2, we outline the components of our P&B algorithm in the next section.

4.2. Price-and-branch

Algorithm 1 shows a pseudocode of our P&B approach. Contrary to B&P where we iterate between pricing and branching, in P&B we price once and then enforce integer feasible solutions without generating new columns. Algorithm 1 solves the continuous relaxation of the given path-based formulation (1. 1) via CG with partial pricing. More specifically, the algorithm initializes a restricted master problem (RMP) (1. 2), and then iteratively solves the RMP (1. 5) and a pricing problem (1. 6) in order to add new columns (1. 7) to the RMP. Every 5 iterations, we enhance the partial pricing by conducting a full pricing iteration that allows to update not only the upper bound (1. 8), but also the lower bound (1. 9-10). After the CG has converged or the time limit has been reached (1. 4), the algorithm branches on the obtained continuous solution in order to enforce integer feasible solutions (1. 13). In the following paragraphs, we detail each algorithmic component.

Restricted master problem: The CG procedure in our algorithm solves the continuous relaxation of Problem 2. However, in Problem 2 the number of feasible paths per request $r \in \mathcal{R}^F$ is intractable even for medium-sized networks. Accordingly, we solve the RMP considering only a subset of these paths, i.e., a subset of $\tilde{\mathcal{P}}(r) \subseteq \mathcal{P}(r)$, $r \in \mathcal{R}^F$. Therefore, we initialize the RMP such that the problem is feasible in the very first iteration of the CG. Specifically, we initialize $\tilde{\mathcal{P}}(r) := \{((o^r, e^r), (d^r, l^r))\}$, $r \in \mathcal{R}^F$. Thus, in the initial solution to the RMP all freight requests are rejected, i.e., sent via their dummy arcs. Then, we add additional variables z_p^r , $r \in \mathcal{R}^F$, $p \in \tilde{\mathcal{P}}(r)$ dynamically until the algorithm terminates. We solve the RMP with a standard commercial solver by warmstarting from the solution of the previous CG iteration.

Pricing problems: The pricing problems identify the variables z_p^r , $r \in \mathcal{R}^F$, $p \in \tilde{\mathcal{P}}(r)$ that we add to the RMP. In every pricing problem, we identify a variable z that represents the

Algorithm 1 Price-and-branch

Require: Path-based formulation (2)

- 1: `relaxation` \leftarrow `ContinuousRelaxation`
- 2: `rmp` \leftarrow `InitializeRMP(relaxation)` ▷ Ensures feasibility throughout CG
- 3: `LB, UB` \leftarrow `0, ∞`
- 4: **while** `OptimalityGap` $>$ ϵ and `SolveTime` $>$ `0` **do**
- 5: `duals` \leftarrow `SolveRMP(rmp)` ▷ Warmstarting at previous solution
- 6: `cols` \leftarrow `Price(duals)`
- 7: `rmp` \leftarrow `AddColumns(rmp, cols)`
- 8: `UB` \leftarrow `UpdateBounds(rmp)` ▷ Solution value of RMP
- 9: **if** `FullPricingIteration` **then** ▷ No update in partial pricing iterations
- 10: `LB` \leftarrow `UpdateBounds(rmp, duals)`
- 11: **end if**
- 12: **end while**
- 13: `solution` \leftarrow `BranchAndCut(rmp)` ▷ No further updates of lower bound
- 14: **return** `solution`

column yielding the maximum primal solution value improvement, and therefore comes with the smallest reduced cost for a given request. The exact solution to the pricing problem is required to obtain valid lower bounds and the reduced cost of a variable depends on the dual problem. To this end, the dual problem of the continuous relaxation of Problem 2 is

$$\begin{aligned} \max_{\gamma, \alpha, \nu, \nu, \delta, \pi, \tau, \eta} \quad & \sum_{r \in \mathcal{R}^P} (\chi q^r \gamma + \delta^r) + \sum_{r \in \mathcal{R}^F} \eta^r + \sum_{h \in \mathcal{H}} \kappa_h \tau_h \\ & + \sum_{(i,j) \in \mathcal{I}} \sum_{h \in \mathcal{H}} \omega_{i,j}^h \lambda_h \kappa_h \nu_{i,j} + \sum_{(i,j) \in \mathcal{J}} \sum_{h \in \mathcal{H}} \omega_{i,j}^h \lambda_h \kappa_h \nu_{i,j} \end{aligned} \quad (3a)$$

s.t.

$$(y) \quad \tau_h - \sum_{(i,j) \in \mathcal{A}^F} \omega_{i,j}^h \pi_{i,j} \leq c_h, \quad \forall h \in \mathcal{H}, \quad (3b)$$

$$(z) \quad \eta^r + \sum_{(i,j) \in \mathcal{A}^F} q^r \theta_{i,j}^p \alpha_{i,j} \leq \sum_{(i,j) \in \mathcal{A}^C} q^r c_{i,j} \theta_{i,j}^p, \quad \forall r \in \mathcal{R}^F, p \in \mathcal{P}(r), \quad (3c)$$

$$(g) \quad q^r \gamma + \delta^r + \sum_{(i,j) \in \mathcal{I}} q^r \theta_{i,j}^p \nu_{i,j} + \sum_{(i,j) \in \mathcal{J}} q^r \theta_{i,j}^p \nu_{i,j} \leq 0, \quad \forall r \in \mathcal{R}^P, p \in \mathcal{P}(r), \quad (3d)$$

$$(x) \quad \pi_{i,j} - \alpha_{i,j} \sum_{h \in \mathcal{H}} \omega_{i,j}^h \lambda_h + \sum_{(i',j') \in \mathcal{G}(i,j)} \nu_{i',j'} \sum_{h \in \mathcal{H}} \omega_{i,j}^h \lambda_h \leq 0, \quad \forall (i,j) \in \mathcal{A}^F, \quad (3e)$$

$$\gamma \geq 0; \quad \alpha, \nu, \nu, \delta, \pi, \tau \leq 0; \quad \eta \text{ free} \quad (3f)$$

where $\mathcal{G}(i,j) := \{(i',j') \in \mathcal{A}^V : \mu(i',j') = (i,j)\}$ denotes the set of all vehicle layer arcs that are contracted into the given freight path segment $(i,j) \in \mathcal{A}^F$. Then, we obtain the respective reduced cost by re-arranging Constraints 3c:

$$\bar{c}_p^r = q^r \left[\sum_{(i,j) \in \mathcal{C}} \theta_{i,j}^p c_{i,j} - \sum_{(i,j) \in \mathcal{A}^F} \theta_{i,j}^p \alpha_{i,j} \right] - \eta^r, \quad \forall r \in \mathcal{R}^F, p \in \mathcal{P}(r) \quad (4)$$

and the corresponding pricing problems for every $r \in \mathcal{R}^F$ are independent and read

$$\min_f \quad q^r \left[\sum_{(i,j) \in \mathcal{A}^C} c_{i,j} f_{i,j}^r - \sum_{(i,j) \in \mathcal{A}^F} \alpha_{i,j} f_{i,j}^r \right] - \eta^r \quad (5a)$$

$$\text{s.t.} \quad \sum_{j \in \mathcal{N}^+(i)} f_{i,j}^r - \sum_{j \in \mathcal{N}^-(i)} f_{j,i}^r = \xi_i^r \quad \forall i \in \mathcal{O} \cup \mathcal{D} \cup \mathcal{B}, \quad (5b)$$

$$f_{i,j}^r \in \{0, 1\}, \quad \forall (i,j) \in \mathcal{A}^C \quad (5c)$$

Solving the pricing problems 5 is equivalent to solving a SPP with adapted arc costs $c_{i,j} - \alpha_{i,j}$, $(i,j) \in \mathcal{A}^F$ on the subgraph of G that is defined by the arc set \mathcal{A}^C for every freight request. Note that the decomposed structure of the pricing problems allows their parallel computation. We can solve these SPPs by standard approaches such as Dijkstra's algorithm, or, more efficiently, with the A* algorithm which is a label setting algorithm that prioritizes paths that are more likely to be optimal and thereby reduces unnecessary exploration. However, A* requires an admissible distance approximation which we can find

from computing SPPs on the unexpanded network, i.e., by discarding the problem’s time dimension as follows: First, we compute lower bounds to the total cost on the minimum cost path between all pairs of FTs in the unexpanded network. We denote the resulting cost mapping as a function $w' : \mathcal{Q} \times \mathcal{Q} \rightarrow [0, \infty)$. Due to the static nature of this cost mapping, we can compute it once in an offline fashion and use it in all pricing iterations. Finally, we complete the computation of the distance approximation w by finding the connection of the request destination representations that yields the lowest approximation of total path cost. Specifically, we determine

$$w(i, j) = \min_{i' \in \mathcal{N}^-(j)} w'(\beta(i), \beta(i')) + c_{i', j}, \forall i \in \mathcal{B}, j \in \mathcal{D}$$

where β maps temporally expanded vertices to their unexpanded representation, i.e., $\beta(v) = s, \forall v = (s, \cdot, \cdot) \in \mathcal{S}$. This gives an admissible distance approximation, which allows us to use the A* algorithm to speed up SPP computations. We refer to Lienkamp & Schiffer (2024) for more details.

Partial pricing: We apply partial pricing and thus, do not solve all pricing problems in every CG iteration. Instead, we only solve a subset of pricing problems in order to reduce computation time and promote heterogeneity in the generated column, which are more likely to be jointly selected in an optimal solution to Problem 2. Formally, we set the pricing strength that determines the maximum number of columns to add per iteration to $\phi \leq 1$. After solving all pricing problems in the first CG iteration, we pop freight requests from the priority queue and solve the corresponding pricing problems until $\phi |\mathcal{R}^F|$ variables with negative reduced cost have been found or all pricing problems have been solved. Here, we maintain the order of requests in the priority queue across pricing iterations. However, we regularly perform a full pricing iteration as suggested in Klein & Schiffer (2023) because partial pricing impedes the computation of tight lower bounds (for a general introduction, see, e.g., Uchoa et al. 2024). Furthermore, we fall back to full pricing iterations if CG convergence slows down and the optimality gap has not improved beyond some threshold for multiple consecutive iterations. Specifically, we compute the average optimality gap reduction over the last 5 iterations and conduct a full pricing iteration if this average reduction is below 0.0001.

Branching: After solving the continuous relaxation of Problem 2 via CG we obtain a solution that is potentially fractional in y, x , and z . We fix the set of variables z to those that are in the current RMP and utilize a commercial solver’s state-of-the-art branch-and-cut implementation to derive an integer feasible solution to Problem 2. By relying on this simple approach, we not only avoid initializing a second model, but effectively provide the solution to the root node of the Branch-and-bound (B&B) by starting the commercial solver at the potentially fractional solution obtained from the CG. Since we generated only a subset of all feasible paths — specifically those required to solve the continuous relaxation at the root node — integer solutions that we obtain while branching remain upper bounds to Problem 1.

4.3. Branch-and-price

As an alternative to our P&B algorithm, we provide a basic B&P approach outlined as shown in Algorithm 2 to find optimal solutions to Problem 2. Contrary to the P&B (cf. Algorithm 1), the B&P algorithm allows to continuously improve the lower bound by iteratively switching between branching and pricing until optimality is proven or a time limit is reached.

Algorithm 2 initializes a queue of active nodes with the continuous relaxation of Problem 2 (l. 2). Then, in every iteration, we pop the first node from this queue and solve its continuous relaxation by CG (l. 4-5). To this end, we apply the same CG with partial pricing as in Algorithm 1. After solving the node, the algorithm first checks if it can prune the search tree based on the obtained solution (l. 6-7). Otherwise, if the obtained solution is fractional in any design variable y , the algorithm derives a node-based upper bound (l. 12). Furthermore, it identifies the design variable to branch based on Equation (6), creates two new child nodes (l. 13), and adds them to the queue of active nodes (l. 14). Two comments are in order. First, we initialize new nodes with a node-based lower bound that equals their parent's lower bound and sort them in the queue accordingly in ascending order. Second, new nodes can be infeasible. We detect infeasibility after popping the node from the queue when solving the RMP in the CG procedure (l. 5) and proceed with the next iteration in this case. If the node-based upper bound derived in Line 12, yields an improvement compared to the solution value of the current incumbent, we update the incumbent and the global upper bound accordingly (l. 16-18). Finally, we update the global lower bound (l. 20) which is given by the minimum node-based lower bounds of all active nodes. In the following, we briefly explain our B&P approach concerning the applied branching rule and the derivation of upper bounds.

Branching strategy: We branch based on the design variables y_h , $h \in \mathcal{H}$ and select the design variable with the highest fractional value in the final solution of the CG applied to

Algorithm 2 Branch-and-price

Require: Path-based formulation (2)

```

1: GlobalLB, GlobalUB, Incumbent  $\leftarrow 0, \infty, \text{None}$ 
2: ActiveNodeQueue  $\leftarrow \text{InitializeNodeQueue}(\text{ContinuousRelaxation})$ 
3: while OptimalityGap  $> \epsilon$  and SolveTime  $> 0$  do
4:   node  $\leftarrow \text{ActiveNodeQueue.pop}()$  ▷ Sorted by parent's lower bound
5:   ContinuousSolution  $\leftarrow \text{ColumnGeneration}(\text{node})$ 
6:   if ContinuousSolution.value  $\geq$  GlobalUB then
7:     continue ▷ Prune search tree
8:   end if
9:   if IsFractional(ContinuousSolution) then
10:    IntegerSolution  $\leftarrow \text{ContinuousSolution}$ 
11:   else
12:    IntegerSolution  $\leftarrow \text{NodeUpperBound}(\text{ContinuousSolution})$  ▷ By standard solver
13:    Left, Right  $\leftarrow \text{BranchingRule}(\text{ContinuousSolution})$  ▷ cf. Equation (6)
14:    ActiveNodeQueue.push(Left, Right)
15:   end if
16:   if IntegerSolution.value  $<$  GlobalUB then
17:     Incumbent  $\leftarrow \text{IntegerSolution}$ 
18:     GlobalUB  $\leftarrow \text{Incumbent.value}$ 
19:   end if
20:   GlobalLB  $\leftarrow \text{UpdateLB}(\text{ContinuousSolution}, \text{ActiveNodeQueue})$  ▷ Min. across active nodes
21: end while
22: return Incumbent

```

solve the continuous relaxation of the respective search tree node. More specifically, after solving a node in the search tree, we determine

$$\arg \max_{y_h, h \in \mathcal{H}} \min\{y_h - \lfloor y_h \rfloor, 1 - (y_h - \lfloor y_h \rfloor)\} \quad (6)$$

and add an inequality to the RMP that reflects the branching. This branching on the design variables does not change the pricing problem. We populate columns found in any search tree node to all currently active nodes and do not prune the set of columns.

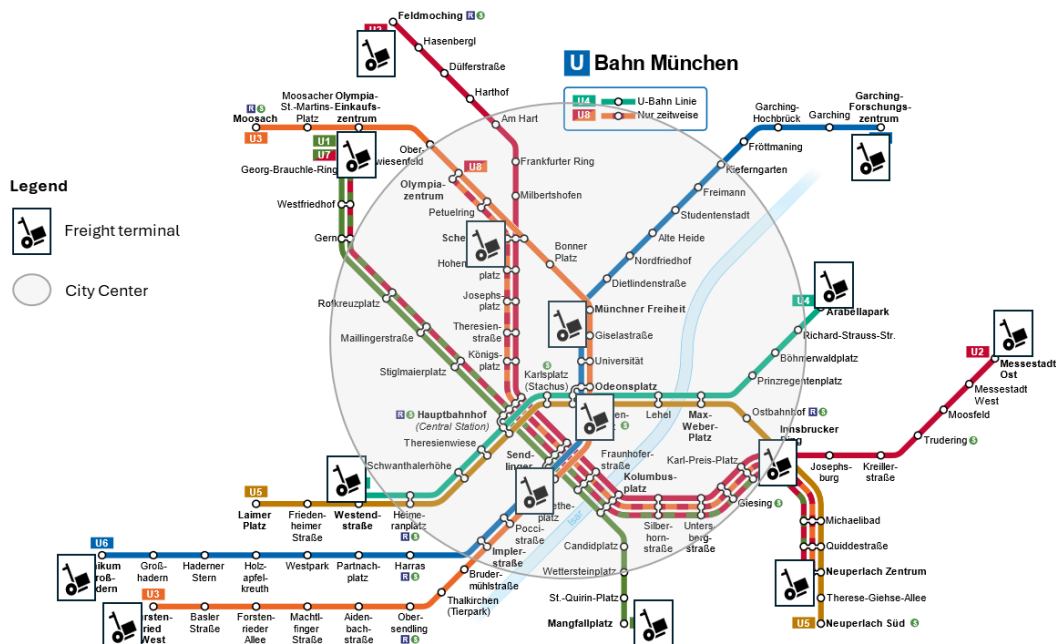
Node-based upper bounds: Following the observation that commercial solvers are capable of branching on a continuous solution of Problem 2 effectively, we assign a restrictive time limit to the commercial solver (e.g., 60 seconds) and utilize its branch-and-cut algorithm to derive upper bounds in every node of the search tree.

5. Experimental design

We test our algorithm on the subway network of Munich (cf. Figure 6) that we enrich by an assumption about the FT layout, and generate instances based on publicly available data where possible.

In the following, we describe our case study and summarize the sources used and the resulting parameters in Table 3. Following the General Transit Feed Specification (GTFS) for the Munich subway network, trip data includes physical locations and timetable information. We concatenate trips from a representative day to reach a reasonable assumption on PT vehicles' routes through the network during the considered time period. Specifically, we assume that two trips are performed by the same vehicle if they end and start at the same PT stop, and no other trip starts or ends at the same stop in the time between the two

Figure 6: Munich subway network (Heilmaier 2020) with assumed FT layout



considered vehicles. Based on information by the operator (MVG 2023), we set heterogeneous vehicle capacities from $\{870, 910, 936\}$ by randomly assigning vehicle types according to the probabilities $\{0.52, 0.13, 0.35\}$ that reflect the current vehicle type distribution in Munich’s PTS.

We sample passenger requests between 6 a.m. and 11 a.m. based on the urban travel demand simulation tool MITO (cf. Moeckel et al. 2020). Here, we scale the demand per passenger request to $q^r = 24.71$, $r \in \mathcal{R}^P$ such that the complete set of 10,000 sampled requests represents the demand in the evaluated time period, which we derive based on the operator’s data for an entire year (cf. MVG 2023). We pre-compute passengers’ potential paths as described in Section 3.2.

Real-world data on urban freight shipments is notoriously hard to get. As an alternative, we sample freight request destination locations based on the population distribution and income per capita distribution per city district and assume that every freight request originates in one of 20 randomly located LSP distribution centers in the city’s outskirts. In this context, we assume that the city’s outskirts lie within a radius of 8-10 km of the city center. We set the homogeneous demand of freight requests such that the accumulated demand reflects the daily parcel delivery volume in Munich derived based on volume per capita (cf. Table 3). To convert the resulting freight demand (in number of parcels) to passenger equivalents, we convert 12 parcels to 1 passenger equivalent. This conversion is based on the required space per passenger, the dimensions of a trolley, the parcel volume, and a trolley utilization of 75%. Furthermore, we connect every origin and destination representation to $\iota = 1$ FT representation as outlined in Section D. Finally, we parameterize costs as follows. First, we derive the daily present value of the total network design cost per HTU of 1.51×10^6 based on 25 years of usage and a current base rate of 3.62%. Specifically, $c_h = \frac{1.51 \times 10^6}{25 \times 365 \times (1 + 0.0362)^{25}} = 68.18 \text{ €}$, $h \in \mathcal{H}$.

Let the externality cost of conventional truck-based delivery be 0.2 € per vehicle and kilometer. Furthermore, we assume a truck tour length of 80 km and a delivery capacity of 100 parcels per tour. According to the conversion factor that we assume, a unit of demand equals 12 parcels. Thus, we set $c_{\text{PEN}}^r = \frac{0.2 \times 80 \times q_r \times 12}{100}$, $r \in \mathcal{R}^F$. Similarly, let the externality cost of

Table 3: Case Study Parameters

Parameter	Unit	Value	Source
Subway passenger demand	passengers/year	353 Mio	MVG (2023)
German parcel volume	parcels/year	4220 Mio	Bundesnetzagentur (2022)
Design cost per HTU	€/HTU	1.515 Mio	MVG (2020)
Externality cost (truck)	€/vehicle & km	[0.05, 11.71]	De Langhe (2017)
Externality cost (cargo bike ^a)	€/vehicle & km	0.115	Schröder et al. (2023)
Subway capacity	Passengers/vehicle	{870, 912, 936}	MVG (2023)
Passenger space requirement	m ²	0.25	VDV (1990)
Duration of fleet usage	years	25	Ger. Fed. Ministry of Finance (2024)
Base rate	%	3.62	Ger. Fed. Bank (2024)
Truck typical tour length	km	80	Oliver Wyman (2021)
Truck capacity	parcels/vehicle	100	Oliver Wyman (2021)
Cargo-Bike typical tour length	km	12.2	Koning & Conway (2016)
Cargo-Bike capacity	parcels/vehicle	20	Llorca & Moeckel (2021)
Parcel volume	m ³	0.027	DHL Paket GmbH (2024)
Trolley dimensions (H x W x D)	m	$1.8 \times 1.2 \times 0.8$	Wanzl GmbH & Co. KGaA (2024)
Working days per year	days	255	-

^aWe assume similar externality cost as for electric mopeds

cargo-bike delivery be 0.115 € per vehicle and kilometer, the average tour length be 12.2 km, and the delivery capacity be 20 parcels per tour. Then, we set $c_{i,j} = \frac{0.115 \times 12.2 \times 12}{20}$, $(i, j) \in \mathcal{A}^E$.

Third, we chose the routing cost $c_{i,j} = 0.0406 \times d_{i,j}$, $(i, j) \in \mathcal{A}^V$ proportionally to the kilometers of distance $d_{i,j}$ between the stops that i and j represent, scaled by the externality cost of the transported freight. All instances share the PTS network and passenger demand. The sizes of the instances differ by the number of freight requests we consider, and we generate $n = 15$ experiments with different seeds for every instance size. Specifically, we generate instances of the sizes $|\mathcal{R}^F| \in [250, 500, 1,000, 2,000, 3,000]$.

All experiments have been conducted single-threaded on a standard desktop computer with an Intel Core i9-9900, 3.1 GHz CPU, and 16 GB of RAM, running Ubuntu 20.04. We have used Python 3.10.2 with CPLEX 22.1 to solve the RMP in the CG and perform the subsequent branching. We used the DOcplex library as a modelling interface, allow CPLEX to use its presolve capabilities, and configure CPLEX to scale the coefficient matrix aggressively in the RMP of the P&B algorithm. We have run all experiments with a maximum runtime of 90 minutes. In our P&B algorithm, we reserve 15 minutes for the branching and stop the CG otherwise at an optimality tolerance of $\epsilon = 0.001$.

6. Results

In the following Section 6.1, we show the efficiency of our algorithmic framework. In this context, we determine the value of partial pricing by providing results with partial pricing of varying degree, i.e., varying number of pricing problems solved per iteration. We show that partial pricing decreases the required number of pricing iterations. Furthermore, we compare our P&B algorithm to a MIP and show that we increase the solvable instance size significantly. Moreover, we provide results of the presented B&P algorithm. In Section 6.2, we present a sensitivity analysis on unknown cost factors, and show that our framework successfully increases the utilization of Munich’s PTS during off-peak hours as well as its capability to allocate capacity in a dynamic fashion respecting passenger demand peaks and scheduling freight transportation around those peaks.

6.1. Computational results

We run our P&B approach with partial pricing and show the value of partial pricing in Table 4 by comparing different pricing strength parameters $\phi \in \{0.1, 0.2, 0.3, 0.4, 0.5, 1.0\}$. As can be seen, solving only 10% of all pricing problems (i.e., $\phi = 0.1$) yields solutions with a median integrality gap below 1.02%. At the same time, partial pricing with $\phi = 0.1$ saves the creation of every second path variable compared to an approach with full pricing, i.e., $\phi = 1.0$. We observe results that are similar in quality but require our algorithm to generate significantly less path variables. This result indicates that partial pricing indeed leads to more heterogeneous columns that are more likely to be jointly selected in an integer solution. We display the distribution of integrality gaps across different instance sizes and pricing strengths in Appendix B.

Table 4: The value of partial pricing ($n = 15$)

Instance Sizes	$\phi = 0.1$	$\phi = 0.2$	$\phi = 0.3$	$\phi = 0.4$	$\phi = 0.5$	$\phi = 1.0$
Median number of variables added per request						
250	22.73	22.94	27.26	32.01	36.58	39.00
500	16.58	20.58	23.59	28.69	33.95	36.88
1,000	15.33	20.10	25.17	30.79	33.12	38.90
2,000	16.18	20.27	24.42	32.47	35.75	40.13
3,000	13.96	19.57	23.39	28.60	31.98	37.48
Median integrality gap						
250	1.02%	0.99%	1.00%	0.98%	0.98%	0.98%
500	0.82%	0.91%	0.77%	0.83%	0.80%	0.83%
1,000	0.84%	0.86%	0.78%	0.75%	0.75%	0.65%
2,000	0.86%	0.93%	0.91%	0.73%	0.75%	0.63%
3,000	1.00%	0.99%	1.02%	0.72%	0.72%	0.62%

Result 1. *Partial pricing increases the heterogeneity of paths such that the number of generated columns decreases from 39.00 to 22.73 in small instances and from 37.48 to 13.96 in large instances while the median integrality gaps are less than 1.02% in all instances.*

Table 5 compares the P&B with the MIP 1 and Figure 7 provides a complementary visualization of the reported integrality gaps and solve times. In this setting, the commercial solver benefits from the presented preprocessing techniques and the implemented graph pruning to the same extent as our P&B algorithm. Solving MIP 1 in a large-scale setting is time-consuming and runs into memory bounds quickly. In particular, while the commercial solver provides a solution with a median integrality gap of less than 1% for all instances of size 250 freight requests and most instances of size 500 freight requests, it consistently runs into memory bounds when extending the setting to a larger scale. Here, we exclude instances that the commercial solver cannot solve from the reported result. Contrary, our P&B approach solves all sets of instances to a median integrality gap of less than 1% within the given time limit and the median solve time to find the first integer feasible solution was 1,286.11 seconds even for the large instances. Figure 7a and Figure 7b show that both results are reasonably stable versus outliers. Specifically, the P&B approach consistently yields solutions below 2%

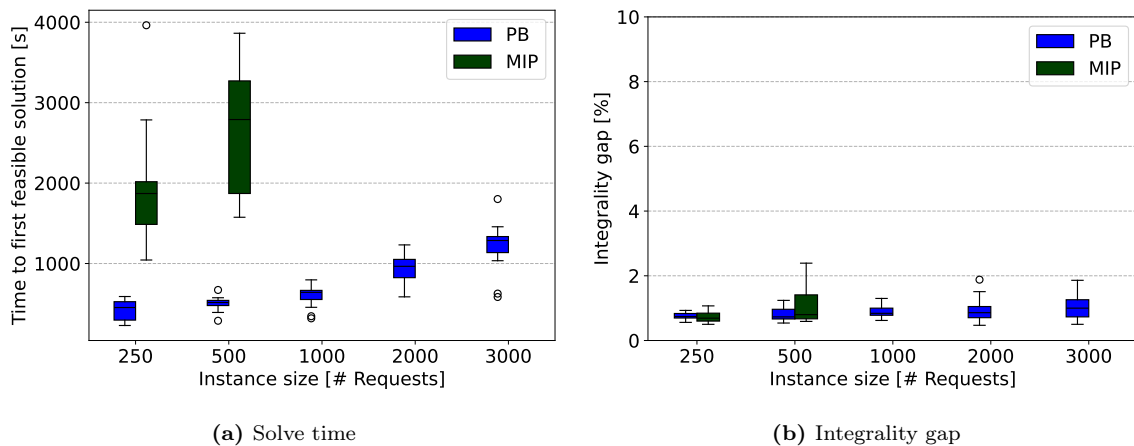
Figure 7: Computational results for P&B

Table 5: Benchmark Results ($n = 15$)

Instance size	Median integrality gap [%]		Median solve time until first feasible solution [s]		Solved instances	
	MIP	P&B	MIP	P&B	MIP	P&B
250	0.69%	0.74%	1,870.40	452.71	15	15
500	0.80%	0.73%	2,790.19	515.07	13	15
1,000	-	0.84%	-	641.31	0	15
2,000	-	0.86%	-	965.17	0	15
3,000	-	1.00%	-	1286.11	0	15

integrality gap for all instances and it takes a maximum of less than 2,000 seconds to find feasible solutions.

Result 2. *Our algorithmic framework with a P&B approach solves larger instances than our algorithmic framework with a commercial solver. The difference in solvable instance sizes reaches a factor of 6, i.e., increases from 500 to 3,000 freight requests.*

In Table 6, we compare our P&B with the B&P algorithm within our algorithmic framework. We report medium, minimum and maximum integrality gaps remaining after 90 minutes for both algorithms.

The B&P approach decreases the integrality gap to smaller values than the P&B approach. However, the P&B yields solutions almost as good as the B&P approach with much less computational effort. The difference of 0.15–0.41 percentage points in the median integrality gaps is marginal due to the low integrality gaps in general. Note that the integrality gaps reported for the P&B in Table 6 differ from the ones previously reported in Table 5. This effect occurs because in Table 5, we compute the gap based on the tightest lower bound found with either the commercial solver or the P&B approach. Because of the good performance of P&B and the significantly increased computational effort stemming from repeatedly branching and pricing, we presented our algorithmic framework focusing on the P&B approach.

Result 3. *Replacing the P&B algorithm with a full B&P algorithm in our algorithmic framework improves median integrality gaps by 0.15 — 0.45 percentage points.*

6.2. Managerial insights

The acceptance of a request by the municipality depends on the relation between transportation costs of the request in the PTS and penalty costs for rejection. The transportation cost in the PTS, on the one hand, depends on the externality cost associated with loading and unloading operations. On the other hand, the penalty cost of rejecting a request depends on the externality costs of truck based delivery. In our base case scenario, we set the arc cost on the transit arcs as $c_{i,j} = 0.1$, $(i, j) \in \mathcal{A}^T$ and the externality cost for truck based delivery to be 0.2 € per vehicle and kilometer.

In our base case with 3,000 freight requests, we obtain a freight request rejection rate of 35.1% rejection rate (see Figure 8a). In the following, we discuss the characteristics of this base case in comparison to two extreme scenarios: an optimistic scenario with truck delivery costs of 0.4€ and $c_{i,j} = 0.1$, $(i, j) \in \mathcal{A}^T$ that favors the acceptance of freight deliveries

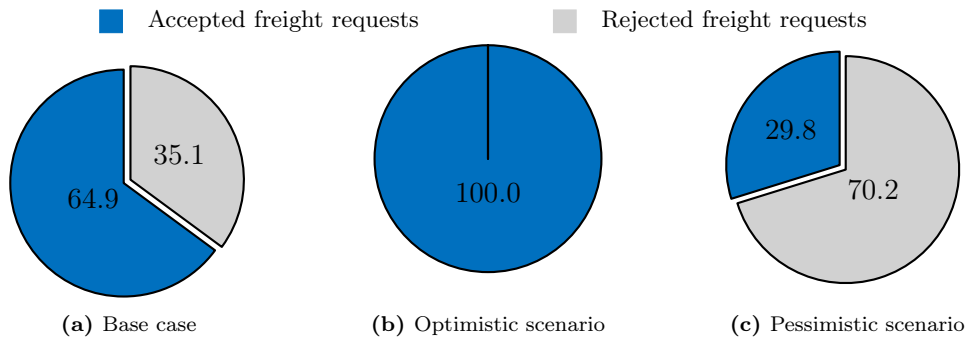
Table 6: B&P and P&B integrality gap results ($n = 15$)

Instance size	B&P integrality gap			P&B integrality gap		
	Median	Min.	Max.	Median	Min.	Max.
250	0.87%	0.73%	0.97%	1.02%	0.86%	1.18%
500	0.62%	0.33%	0.75%	0.82%	0.68%	1.32%
1,000	0.49%	0.28%	0.72%	0.84%	0.62%	1.30%
2,000	0.45%	0.22%	1.03%	0.86%	0.47%	1.88%
3,000	0.65%	0.18%	1.21%	1.00%	0.50%	1.86%

(see Figure 8b), as well as a pessimistic scenario with truck delivery costs of 0.2 € and $c_{i,j} = 0.2$, $(i, j) \in \mathcal{A}^T$ that reduces the acceptance of freight deliveries (see Figure 8c). In the following, we analyze system characteristics for these three cases in Figure 9 before providing a more granular analysis on the respective cost trade-off in Table 7.

Figure 9 details the system utilization for the three scenarios mentioned above, focusing on the system’s utilization over time (Figure 9a), the system’s spatial utilization (Figure 9b), as well as the utilization per vehicle over time for one representative vehicle (Figure 9c). Focusing on the system’s utilization over time, Figure 9a shows the share of freight requests and passengers in the system with respect to the overall amount of requests and passengers in the respective scenario. To visualize the systems dynamics accurately, we exclude idle requests from this visualization. Since passenger flows are prioritized over freight requests and are constrained in time and alternative paths, the passenger utilization shows a similar pattern in all three scenarios, exhibiting a typical commuter peak around 8am. For the system’s freight utilization, we observe different dynamics across all scenarios: in the base case, the freight utilization ranges constantly between 4% and 8% during most of the time horizon, showing slightly elevated utilizations before and after the passenger utilization peak. In the optimistic scenario, we try to push as much freight as possible through the system but are limited by its capacity constraints, i.e., the additional passenger flow that occupies transport volume and is prioritized over the freight requests. Accordingly, we observe a drop in freight utilization at the beginning of the passenger peak, and an additional peak in freight utilization once the passenger peak declines. In the pessimistic scenario, we observe a significantly reduced freight utilization that stems from the shifted cost ratio; although additional transport capacity is available in the system it is cost-optimal to leave the freight requests to conventional truck-based delivery.

Figures 9b and 9c detail the impact of these flow volumes for the most utilized legs in the PTS and a representative vehicle. As can be seen, the utilization related to freight requests in certain network legs scales with the overall utilization in the system (see Figure 9b). Still, we observe classical bottle neck effects as the utilization on Leg IV-VIII is significantly higher than all other utilizations across all scenarios. From a microscopic perspective at vehicle level, we observe that the passenger utilization curve shows multiple peaks in a frequency of around 0.5 hours (see Figure 9c). These peaks stem from the vehicles trajectory, going back and forth on its line: the vehicle frequently crosses the vaster city center area but is less

Figure 8: Cargo-hitching penetration across different scenarios

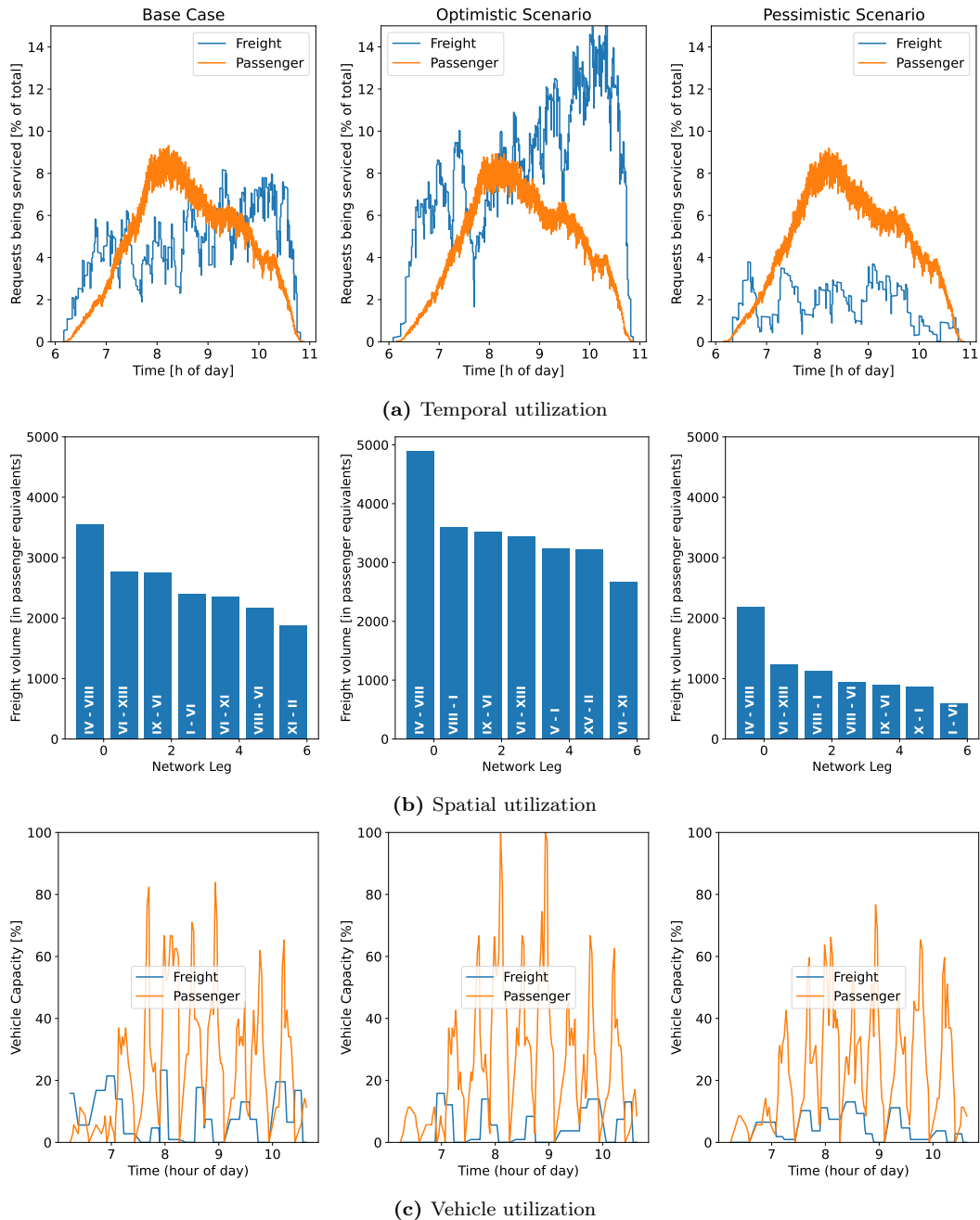
utilized around the turnaround points. As can be seen, our algorithm determines a solution that routes freight through the network utilizing the available excess capacity of the vehicle. The beneficial effect of dynamically allocating capacity is particularly evident in this plot at around 9am when passengers almost fully utilize the vehicle, and no additional freight is transported. Particularly the optimistic scenario demonstrates the importance of dynamic capacity allocation, as the displayed vehicle utilizes its entire capacity for passenger transit demand at around 8am and 9am. Nevertheless, when its capacity is not fully required for passengers, it repeatedly transports freight.

Result 4. *Cargo-hitching offers a utilization increase at zero additional installed capacity, and our algorithmic framework provides solutions that predominantly utilize the PTS's off-peak hours to transport freight requests, leading to higher overall utilizations.*

Abstracting from the scenarios analyzed in Figure 9, it becomes evident that the potential savings that can be realized by cargo-hitching depend on the spare capacity left within the PTS as well as the amount of freight requests that can be shipped through it. In this context, relying on HTUs to realize cargo-hitching is particularly beneficial if the amount of freight requests is high but the spare capacity left in the PTS fluctuates over the day due to passenger flow peaks.

Beyond these general findings, the amount of freight requests transported through the PTS is sensitive to the loading and unloading cost as well as the externality cost of truck-based deliveries. Table 7 shows this trade-off and its impact on the share of rejected freight requests. At an externality cost of truck-based delivery per vehicle and kilometer of 0.05 €, which constitutes the lower bound reported in the literature, the acceptance of cargo-hitching vanishes and all requests are rejected by the municipality. On the other hand, rejection rates diminish at higher penalty costs driven by higher externality costs from truck-based deliveries. As can be seen, at penalty costs resulting from an externality cost of truck-based transport of 1.6 € per vehicle and kilometer, the municipality accepts all requests.

Result 5. *At an externality cost of 1.6 € per vehicle and kilometer, cargo-hitching reaches full penetration if the cost for loading and unloading is less than 2 € per passenger equivalent unit.*

Figure 9: System utilization

I: Sendlinger Tor, II: Scheidplatz, III: Garching, Forschungszentrum, IV: Neuperlach Zentrum, V: Klinikum Großhadern, VI: Odeonsplatz, VII: Mangfallplatz, VIII: Innsbrucker Ring, IX: Arabellapark, X: Olympia-Einkaufszentrum, XI: Münchner Freiheit, XII: Messestadt Ost, XIII: Westendstraße, XIV: Fürstenried West, XV: Feldmoching

Focusing on a broader interpretation of Table 7, we observe that rejection rates above the diagonal are low. This general observation indicates that the penetration of the concept is highly correlated with the direct comparison between the externality cost for truck-based delivery and the cost for loading and unloading represented by the respective arc cost factor.

Table 7: Average share of rejected requests depending on externality cost

$c_{i,j},$ $(i,j) \in \mathcal{A}^T$	Externality cost (Truck) [EUR per vehicle and kilometer]								
	0.05	0.20	0.40	0.60	0.80	1.00	1.20	1.40	1.60
0.1	1.000	0.351	0.000	0.000	0.000	0.000	0.000	0.000	0.000
0.2	1.000	0.702	0.000	0.000	0.000	0.000	0.000	0.000	0.000
0.3	1.000	0.809	0.001	0.000	0.000	0.000	0.000	0.000	0.000
0.4	1.000	0.930	0.021	0.000	0.000	0.000	0.000	0.000	0.000
0.5	1.000	0.933	0.089	0.000	0.000	0.000	0.000	0.000	0.000
0.6	1.000	0.933	0.452	0.000	0.000	0.000	0.000	0.000	0.002
0.8	1.000	0.933	0.636	0.054	0.000	0.000	0.000	0.000	0.000
1.0	1.000	0.933	0.642	0.103	0.000	0.000	0.000	0.000	0.000
1.2	1.000	0.933	0.740	0.631	0.054	0.000	0.000	0.000	0.000
1.4	1.000	0.933	0.933	0.631	0.058	0.054	0.000	0.000	0.000
1.6	1.000	0.933	0.933	0.632	0.574	0.054	0.000	0.000	0.000
1.8	1.000	0.933	0.933	0.636	0.630	0.055	0.054	0.000	0.000
2.0	1.000	0.933	0.933	0.655	0.631	0.230	0.054	0.017	0.000

7. Conclusion

We introduced the urban cargo-hitching problem with dynamic allocation of capacity, heterogeneous PT vehicles, and freight transshipments on a state-of-the-art partially time-expanded and spatially-expanded graph. Based on the expanded graph, we provided an algorithmic framework that relies on multiple preprocessing techniques and a P&B algorithm to solve instances with up to 3,000 freight requests, obtaining a median integrality gap of less than 1.02% within computational time of 90 minutes. We further present a B&P algorithm that allows to obtain even smaller optimality gaps of 0.15 – 0.41 percentage points at the price of increased computational cost.

Our results for the subway network of Munich, Germany, indicate that the ratio of externality costs is the determining factor for high penetration rates of the cargo-hitching concept. We conducted a sensitivity analysis on this ratio and found that cargo-hitching is worthwhile if truck-based transport occurs at an externality cost of more than 1.6 € per vehicle and kilometer and loading and unloading costs of less than 2 € per passenger equivalent. Additionally, we showed that our framework increases the PTS utilization with a focus on off-peak hours and enables decision-makers to evaluate the importance of single parts of the evaluated PTS. We show that relying on HTUs to realize cargo-hitching is particularly beneficial if the amount of freight requests is high but the spare capacity left in the PTS fluctuates over the day due to passenger flow peaks.

Our work provides a scalable algorithmic framework that lays the foundation for future work, e.g., by extending it to determine (capacitated) FT locations. In this context, future work may also focus on incorporating stochastic demand patterns to take informed strategic decisions on the respective network design.

References

- Arvidsson, N., & Browne, M. (2013). A review of the success and failure of tram systems to carry urban freight: The implications for a low emission intermodal solution using electric vehicles on trams. *European Transport*, 54.

- Azcuy, I., Agatz, N., & Giesen, R. (2021). Designing integrated urban delivery systems using public transport. *Transportation Research Part E: Logistics and Transportation Review*, *156*, 102525.
- Behiri, W., Belmokhtar-Berraf, S., & Chu, C. (2018). Urban freight transport using passenger rail network: Scientific issues and quantitative analysis. *Transportation Research Part E: Logistics and Transportation Review*, *115*, 227–245.
- Boland, N., Hewitt, M., Marshall, L., & Savelsbergh, M. (2017). The Continuous-Time Service Network Design Problem. *Operations Research*, *65*, 1303–1321.
- Bundesnetzagentur (2022). Paketmarktbericht 2021. Available at <https://www.bundesnetzagentur.de/SharedDocs/Mediathek/Berichte/2022/Paketmarktbericht2021.pdf>, Accessed: 2024-03-14.
- Cheng, G., Guo, D., Shi, J., & Qin, Y. (2018). When Packages Ride a Bus: Towards Efficient City-Wide Package Distribution. In *IEEE 24th International Conference on Parallel and Distributed Systems* (pp. 259–266).
- Chinn, D., Lotz, C., Speksnijder, L., Stern, S., Chapuis, R., Holmes, R., Knol, A., Tadjeddine, K., & Wolfs, K. (2020). Restoring public transit amid COVID-19: What European cities can learn from one another. Available at <https://www.mckinsey.com/industries/travel-logistics-and-infrastructure/our-insights/restoring-public-transit-amid-covid-19-what-european-cities-can-learn-from-one-another>.
- Dablanc, L. (2011). City Distribution, a Key Element of the Urban Economy: Guidelines for Practitioners. In *City Distribution and Urban Freight Transport*. Edward Elgar Publishing.
- Delle Donne, D., Alfandari, L., Archetti, C., & Ljubić, I. (2023). Freight-on-Transit for urban last-mile deliveries: A strategic planning approach. *Transportation Research Part B: Methodological*, *169*, 53–81.
- DHL Paket GmbH (2024). Preisübersicht für den deutschlandweiten Versand. Available at <https://www.dhl.de/de/privatkunden/pakete-versenden/deutschlandweit-versenden/preise-national.html>, Accessed: 2024-04-24.
- Di, Z., Yang, L., Shi, J., Zhou, H., Yang, K., & Gao, Z. (2022). Joint optimization of carriage arrangement and flow control in a metro-based underground logistics system. *Transportation Research Part B: Methodological*, *159*, 1–23.
- El Ouadi, J., Errousso, H., Malhene, N., Benhadou, S., & Medromi, H. (2022). A machine-learning based hybrid algorithm for strategic location of urban bundling hubs to support shared public transport. *Quality & Quantity*, *56*, 3215–3258.
- Elbert, R., & Rentschler, J. (2022). Freight on urban public transportation: A systematic literature review. *Research in Transportation Business & Management*, *45*, 100679.
- Elbert, R., Rentschler, J., & Schwarz, J. (2023). Combined Hub Location and Service Network Design Problem: A Case Study for an Intermodal Rail Operator and Structural Analysis. *Transportation Research Record*, *2677*, 730–740.
- Fatnassi, E., Chaouachi, J., & Klibi, W. (2015). Planning and operating a shared goods and passengers on-demand rapid transit system for sustainable city-logistics. *Transportation Research Part B: Methodological*, *81*, 440–460.
- Fattah, M. A., Morshed, S. R., & Kafy, A.-A. (2022). Insights into the socio-economic impacts of traffic congestion in the port and industrial areas of Chittagong city, Bangladesh. *Transportation Engineering*, *9*, 100122.
- Ger. Fed. Bank (2024). Basiszinssatz nach §247 BGB. Available at <https://www.bundesbank.de/de/bundesbank/organisation/agb-und-regelungen/basiszinssatz-607820>, Accessed: 2024-03-14.
- Ger. Fed. Ministry of Finance (2024). Abschreibungstabelle für allgemein verwendbare Anlagegüter. Available at https://www.bundesfinanzministerium.de/Web/DE/Themen/Steuern/Steuerverwaltung/Steuerrecht/Betriebsprüfung/AfA_Tabellen/afa_tabellen.html, Accessed: 2024-03-14.
- Ghilas, V., Cordeau, J.-F., Demir, E., & Van Woensel, T. (2018). Branch-and-Price for the Pickup and Delivery Problem with Time Windows and Scheduled Lines. *Transportation Science*, *52*, 1191–1210.
- Ghilas, V., Demir, E., & Van Woensel, T. (2016a). An Adaptive Large Neighborhood Search Heuristic for the Pickup and Delivery Problem with Time Windows and Scheduled Lines. *Computers & Operations Research*, *72*, 12–30.
- Ghilas, V., Demir, E., & Van Woensel, T. (2016b). The pickup and delivery problem with time windows and scheduled lines. *INFOR: Information Systems and Operational Research*, Taylor & Francis, *54*, 147–167.
- Ghilas, V., Demir, E., & Van Woensel, T. (2016c). A scenario-based planning for the pickup and delivery problem with time windows, scheduled lines and stochastic demands. *Transportation Research Part B: Methodological*, *91*, 34–51.
- Heilmaier, Z. (2020). Netzplan U-Bahn München. Available at https://de.m.wikipedia.org/wiki/Datei:Netzplan_U-Bahn_München.svg, Accessed: 2024-05-22.
- Hörsting, L., & Cleophas, C. (2023). Scheduling shared passenger and freight transport on a fixed infrastructure. *European Journal of Operational Research*, *306*, 1158–1169.
- Ji, Y., Zheng, Y., Zhao, J., Shen, Y., & Du, Y. (2020). A Multimodal Passenger-and-Package Sharing Network for Urban Logistics. *Journal of Advanced Transportation*, *2020*.

- Kelly, J., & Marinov, M. (2017). Innovative Interior Designs for Urban Freight Distribution Using Light Rail Systems. *Urban Rail Transit*, 3, 238–254.
- Kızıl, K. U., & Yıldız, B. (2023). Public Transport-Based Crowd-Shipping with Backup Transfers. *Transportation Science*, 57, 174–196.
- Klein, P. S., & Schiffer, M. (2023). Electric Vehicle Charge Scheduling with Flexible Service Operations. *Transportation Science*, 57, 1605–1626.
- Koning, M., & Conway, A. (2016). The good impacts of biking for goods: Lessons from Paris city. *Case Studies on Transport Policy*, 4, 259–268.
- De Langhe, K. (2017). The importance of external costs for assessing the potential of trams and trains for urban freight distribution. *Research in Transportation Business & Management*, 24, 114–122.
- Levy, J. I., Buonocore, J. J., & von Stackelberg, K. (2010). Evaluation of the public health impacts of traffic congestion: a health risk assessment. *Environmental Health*, 9, 65.
- Li, S., Zhu, X., Shang, P., Li, T., & Liu, W. (2023). Optimizing a shared freight and passenger high-speed railway system: A multi-commodity flow formulation with benders decomposition solution approach. *Transportation Research Part B: Methodological*, 172, 1–31.
- Li, S., Zhu, X., Shang, P., Wang, L., & Li, T. (2024). Scheduling shared passenger and freight transport for an underground logistics system. *Transportation Research Part B: Methodological*, 183, 102907.
- Lienkamp, B., & Schiffer, M. (2024). Column generation for solving large scale multi-commodity flow problems for passenger transportation. *European Journal of Operational Research*, 314, 703–717.
- Lin, J., & Zhang, F. (2024). Modular vehicle-based transit system for passenger and freight co-modal transportation. *Transportation Research Part C: Emerging Technologies*, 160, 104545.
- Llorca, C., & Moeckel, R. (2021). Assessment of the potential of cargo bikes and electrification for last-mile parcel delivery by means of simulation of urban freight flows. *European Transport Research Review*, 13.
- Ma, M., Zhang, F., Liu, W., & Dixit, V. (2023). On urban co-modality: Non-cooperative and cooperative games among freight forwarder, carrier and transit operator. *Transportation Research Part C: Emerging Technologies*, 153, 104234.
- Machado, B., Pimentel, C., & Sousa, A. d. (2023a). Integration planning of freight deliveries into passenger bus networks: Exact and heuristic algorithms. *Transportation Research Part A: Policy and Practice*, 171, 103645.
- Machado, B., de Sousa, A., & Pimentel, C. (2023b). Optimization of Last Mile Logistics Process Combining Passenger and Freight Flows. In *Quality Innovation and Sustainability* (pp. 347–359). Springer International Publishing.
- Mandal, M. P., & Archetti, C. (2023). A decomposition approach to last mile delivery using public transportation systems. Available at <https://arxiv.org/abs/2306.04219>. Submitted.
- Masson, R., Trentini, A., Lehuédé, F., Malhéné, N., Péton, O., & Tlahig, H. (2017). Optimization of a city logistics transportation system with mixed passengers and goods. *EURO Journal on Transportation and Logistics*, 6, 81–109.
- Moeckel, R., Kuehnel, N., Llorca, C., Moreno, A., & Rayaprolu, H. (2020). Agent-Based Simulation to Improve Policy Sensitivity of Trip-Based Models. *Journal of Advanced Transportation*, 2020, 1902162.
- Mourad, A., Puchinger, J., & Chu, C. (2019). A survey of models and algorithms for optimizing shared mobility. *Transportation Research Part B: Methodological*, 123, 323–346.
- MVG (2020). MVG – Mobilität in München. Available at <https://www.mvg.de/ueber/presse-print/pressemeldungen/2020/juli/2020-07-02-Modernisierungsschub-U-Bahn-weitere-C2.html>, Accessed: 2024-03-14.
- MVG (2023). MVG – Mobilität in München. Available at https://www.mvg.de/dam/mvg/ueber/unternehmensprofil/mvg_in_zahlen_s, Accessed: 2024-03-14.
- Nieto-Isaza, S., Fontaine, P., & Minner, S. (2022). The value of stochastic crowd resources and strategic location of mini-depots for last-mile delivery: A Benders decomposition approach. *Transportation Research Part B: Methodological*, 157, 62–79.
- Noussan, M., Campisi, E., & Jarre, M. (2022). Carbon Intensity of Passenger Transport Modes: A Review of Emission Factors, Their Variability and the Main Drivers. *Sustainability*, 14.
- Oliver Wyman (2021). Is E-Commerce Good for Europe? - Economic and environmental impact study. Available at <https://www.oliverwyman.de/content/dam/oliver-wyman/v2/publications/2021/apr/is-ecommerce-good-for-europe.pdf>, Accessed: 2024-03-14.
- Onomotion GmbH (2021). VGF getestet Gütertransport mit der Strassenbahn. Available at <https://onomotion.com/2021/09/28/vgf-testet-guetertransport-mit-der-strassenbahn/>, Accessed: 2024-08-12.
- Ozturk, O., & Patrick, J. (2018). An optimization model for freight transport using urban rail transit. *European Journal of Operational Research*, 267, 1110–1121.
- Schröder, D., Kirn, L., Kinigadner, J., Loder, A., Blum, P., Xu, Y., & Lienkamp, M. (2023). Ending the myth of mobility at zero costs: An external cost analysis. *Research in Transportation Economics*, 97, 101246.

-
- Trentini, A., & Malhene, N. (2012). Flow Management of Passengers and Goods Coexisting in the Urban Environment: Conceptual and Operational Points of View. *Seventh International Conference on City Logistics*, 39, 807–817.
- Uchoa, E., Pessoa, A., & Moreno, L. (2024). *Optimizing with Column Generation: Advanced Branch-Cut-and-Price Algorithms (Part I)*. Technical Report.
- United Nations (2019). World Urbanization Prospects: The 2018 Revision. Available at <https://population.un.org/wup/Publications/Files/WUP2018-Report.pdf>, Accessed: 2024-03-14.
- VDV (1990). Richtlinie zur Bestimmung des Fassungsvermögens von Fahrzeugen des Personenverkehrs für statistische Zwecke. Available at https://www.mobi-wissen.de/files/platzkilometer_ebene2.pdf, Accessed: 2024-03-14.
- VGF (2021). Gütertram: Demonstrationsfahrt der VGF (press release). Available at <https://www.vgf-fm.de/de/aktuelles/news/einzelansicht/guetertram-demonstrationsfahrt-der-vgf>, Accessed: 2024-03-14.
- Wanzl GmbH & Co. KGaA (2024). Package roll containers - Modular design for individual solutions. Available at https://www.wanzl.com/de_DE/produkte/wagen/rollcontainer/paketrollbehaelter/paketrollbehaelter~p1558, Accessed: 2024-04-24.
- Zhao, L., Li, H., Li, M., Sun, Y., Hu, Q., Mao, S., Li, J., & Xue, J. (2018). Location selection of intra-city distribution hubs in the metro-integrated logistics system. *Tunnelling and Underground Space Technology*, 80, 246–256.

A. Notation

Table 8 provides a summary of notation which is introduced in the main body of the paper.

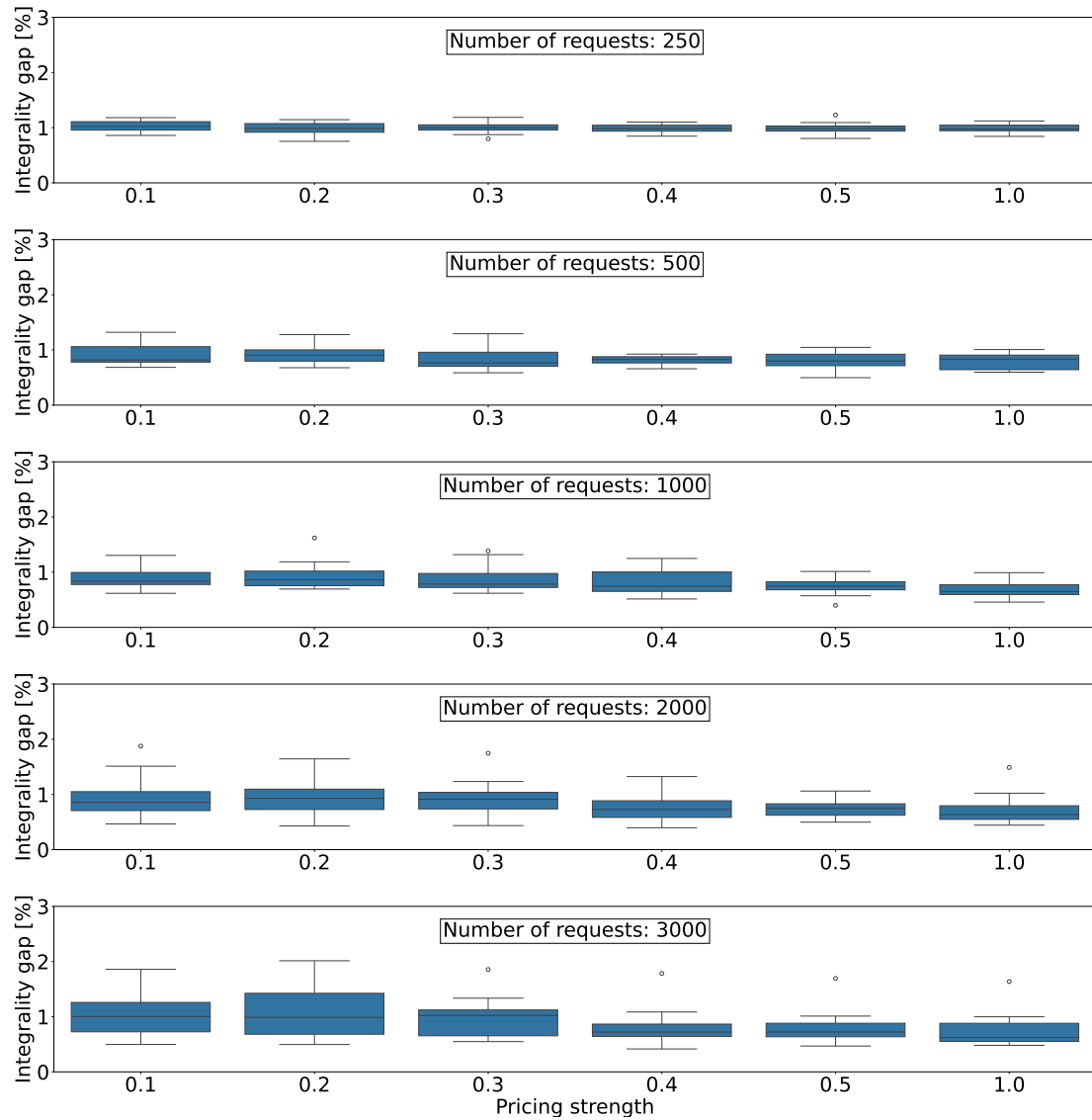
Table 8: Notation

Symbol	Meaning
Basic sets	
$G = (\mathcal{V}, \mathcal{A})$	Expanded, multi-layered, preprocessed and directed graph
\mathcal{P}	Set of valid paths in G
\mathcal{H}	Set of vehicles
\mathcal{R}	Set of requests
Subsets	
$\mathcal{R}^P \subseteq \mathcal{R}$	Set of passenger requests
$\mathcal{R}^F \subseteq \mathcal{R}$	Set of freight requests
$\mathcal{S} \subset \mathcal{V}$	Temporal vertices representing PT stops
$\mathcal{B} \subseteq \mathcal{S}$	Temporal vertices representing FTs
$\mathcal{O} \subset \mathcal{V}$	Temporal vertices representing request origins
$\mathcal{D} \subset \mathcal{V}$	Temporal vertices representing request destinations
$\mathcal{A}^V \subset \mathcal{A}$	Vehicle arcs ($c_{i,j} > 0, \forall (i,j) \in \mathcal{A}^V$)
$\mathcal{A}^F \subset \mathcal{A}$	Freight segments arcs ($c_{i,j} > 0, \forall (i,j) \in \mathcal{A}^F$)
$\mathcal{A}^0 \subset \mathcal{A}$	Holding arcs ($c_{i,j} = 0, \forall (i,j) \in \mathcal{A}^0$)
$\mathcal{A}^T \subset \mathcal{A}$	Transit arcs ($c_{i,j} > 0, \forall (i,j) \in \mathcal{A}^T$)
$\mathcal{A}^D \subset \mathcal{A}$	Dummy arcs ($c_{i,j} > 0, \forall (i,j) \in \mathcal{A}^D$)
$\mathcal{A}^A \subset \mathcal{A}$	Access arcs ($c_{i,j} \geq 0, \forall (i,j) \in \mathcal{A}^A$)
$\mathcal{A}^E \subset \mathcal{A}$	Egress arcs ($c_{i,j} \geq 0, \forall (i,j) \in \mathcal{A}^E$)
Indices	
h	Vehicle $h \in \mathcal{H}$
(i, j)	Arc in $G = (\mathcal{V}, \mathcal{A})$
r	Request $r \in \mathcal{R}$
p	Path $p \in \mathcal{P}$
Variables	
$f_{i,j}^r$	Freight flow of r traversing (i, j)
g_p^r	Passenger flow of r traversing p
y_h	Number of HTUs assigned to h
$x_{i,j}$	Number of HTUs transporting freight on (i, j)
Parameters	
χ	Demand-weighted passenger service level
c_h	Scaled investment cost per HTU with vehicle h
$c_{i,j}$	Cost per unit of flow on arc (i, j)
λ_h	Transportation unit capacity of vehicle h
κ_h	Number of transportation units with vehicle h
Other	
$\mathcal{P}(r) \subseteq \mathcal{P}$	Paths of r
$\mathcal{N}^+(i) / \mathcal{N}^-(i) \subset \mathcal{V}$	Set of neighboring vertices of i (w.r.t. freight)
$\mathcal{A}^C \subseteq \mathcal{A}$	Temporal arcs allowing freight flow
$\theta_{i,j}^p$	1 if path p contains (i, j) , 0 otherwise
$\omega_{i,j}^h$	1 if vehicle h operates arc (i, j) , 0 otherwise
ξ_i^r	Temporal vertex demand at i for request r

B. Partial pricing results

Figure 10 shows the integrality gaps after 90 minutes of our P&B approach for varying instance sizes and pricing strengths.

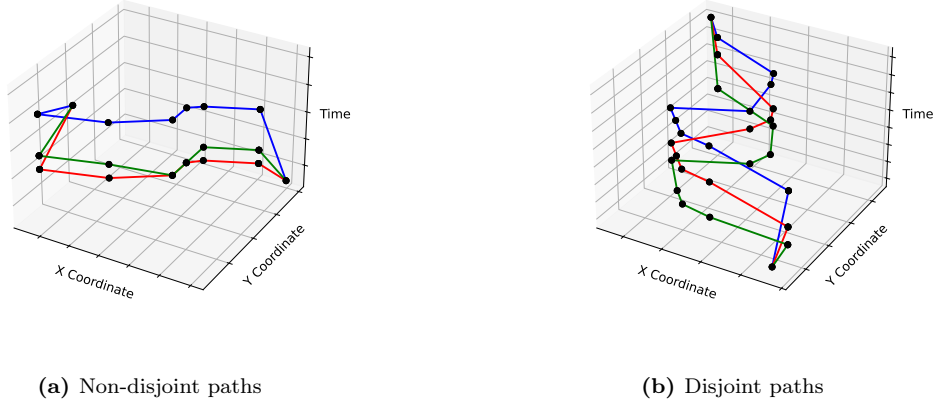
Figure 10: Integrality gaps for varying pricing strengths



C. Exemplary passenger paths

We assume tight service time intervals and argue that passengers prefer convenience, i.e., short travel times. Thus, we compute the shortest paths by travel time for every request. In this context, we purposefully do not compute edge-disjoint paths as this appears to be a hard limitation, especially for requests that start or end at remote locations only connected to the PTS by one single line. In these cases, the computation of disjoint paths would lead to a set of paths that mainly differ in the temporal dimension, and the resulting paths would not offer a choice between equally valued paths from a passenger’s perspective. Furthermore, the network topology of a subway network leads to paths with limited overlap and, in many instances, even to disjoint paths without explicitly enforcing it. Figure 11a demonstrates why we waive the computation of disjoint paths. In this example, two paths are almost edge-disjoint but share a single edge. Figure 11b shows an example where our approach yields edge-disjoint paths.

Figure 11: Exemplary passenger paths



D. Implementation

Two comments on the graph expansion and algorithmic framework implementation are in order.

First, we pre-compute feasible and realistic paths for passenger requests $r \in \mathcal{R}^P$ by computing the three shortest paths with respect to travel time such that the itinerary starts and ends in the given service time interval $[e^r, l^r]$. Here, we assume a reasonable walking speed of 1 m/s on access and egress arcs $(i, j) \in \mathcal{A}^A \cup \mathcal{A}^E$.

Second, we prune the graph G when creating the sets \mathcal{A}^A and \mathcal{A}^E as follows. We remove (o^r, e^r) and $(d^r, l^r), r \in \mathcal{R}^P$ including their incoming and outgoing arcs from graph G because our algorithmic framework does not require them anymore after pre-computing the paths for passenger requests. Instead, we remove the respective components from both the graph G and the pre-computed paths. Furthermore, we only connect $i = (o^r, e^r) \in \mathcal{O}, r \in \mathcal{R}^P$ to a vertex $j = (s, t, 0) \in \mathcal{S}^0$ if

- a) the time difference remains above a certain threshold $\zeta(r), r \in \mathcal{R}^P$ indicating that time suffices to relocate from o^r to s , thus $t - e^r \geq \zeta(r)$
- b) if there exist no earlier representation of the same stop s to which i can be connected while respecting condition a), thus $\nexists (s, t', 0) \in \mathcal{S}^0 : t' < t \wedge t' - e \geq \zeta(r)$
- c) the vertex j represents one of the ι closest FTs in the PTS according to the distance between the represented stop s and the requests origin o^r .

By applying the same reasoning, we prune the temporal arc set \mathcal{A}^E . Hence, we condition the existence of an arc on

- a) $l^r - t \geq \zeta(r)$
- b) the absence of a later representation of the same stop in the holding layer
- c) s being one of the ι closest FTs.

We allow to temporarily store freight at FTs by assigning a zero cost to the arcs in \mathcal{A}^0 . In this context, connecting origins and destinations to the earliest and latest representations of stops reduces the cardinality of the arc set without sacrificing solution quality. We can post-process the solutions to avoid unnecessary long service times due to holding a request at the first or last stop of its path.